

# Methanethiol, dimethyl sulfide and acetone over biologically productive waters in the SW Pacific Ocean

Sarah J. Lawson<sup>1</sup>, Cliff S. Law<sup>2,3</sup>, Mike J. Harvey<sup>2</sup>, Thomas G. Bell<sup>4</sup>, Carolyn F. Walker<sup>2</sup>, Warren J. de Bruyn<sup>5</sup> and Eric S. Saltzman<sup>6</sup>

<sup>1</sup> Commonwealth Scientific and Industrial Research Organisation, Oceans and Atmosphere, Aspendale, Australia

<sup>2</sup> National Institute of Water and Atmospheric Research, Wellington, New Zealand

<sup>3</sup> Dept. Chemistry, University of Otago, Dunedin, New Zealand

<sup>4</sup> Plymouth Marine Laboratory, Plymouth, UK

<sup>5</sup> Schmidt College of Science and Technology, Chapman University, Orange, California, CA, USA

<sup>6</sup> Earth System Science, University of California, Irvine, California, USA

Correspondence to: Sarah J. Lawson ([sarah\\_jane\\_lawson@yahoo.com.au](mailto:sarah_jane_lawson@yahoo.com.au))

## Abstract

Atmospheric methanethiol (MeSH<sub>a</sub>), dimethyl sulfide (DMS<sub>a</sub>) and acetone (acetone<sub>a</sub>) were measured over biologically productive frontal waters in the remote South West Pacific Ocean in summertime 2012 during the Surface Ocean Aerosol Production (SOAP) voyage. MeSH<sub>a</sub> mixing ratios varied from below detection limit (< 10 ppt) up to 65 ppt and were 3 - 36% of parallel DMS<sub>a</sub> mixing ratios. MeSH<sub>a</sub> and DMS<sub>a</sub> were correlated over the voyage ( $R^2=0.3$ , slope=0.07) with a stronger correlation over a coccolithophore-dominated phytoplankton bloom ( $R^2=0.5$ , slope 0.13). The diurnal cycle for MeSH<sub>a</sub> shows similar behaviour to DMS<sub>a</sub> with mixing ratios varying by a factor of ~2 according to time of day with the minimum levels of both MeSH<sub>a</sub> and DMS<sub>a</sub> occurring at around 16:00 hrs local time. A positive flux of MeSH out of the ocean was calculated for 3 different nights and ranged from 3.5 - 5.8  $\mu\text{mol m}^{-2} \text{ day}^{-1}$  corresponding to 14 - 24% of the DMS flux (MeSH/(MeSH+DMS)). Spearman rank correlations with ocean biogeochemical parameters showed a moderate to strong positive and highly significant relationship between both MeSH<sub>a</sub> and DMS<sub>a</sub> with seawater DMS (DMS<sub>sw</sub>), and a moderate correlation with total dimethylsulfoniopropionate (total DMSP). A positive correlation of acetone<sub>a</sub> with water temperature and negative correlation with nutrient concentrations is consistent with reports of acetone production in warmer subtropical waters. Positive correlations of acetone<sub>a</sub> with cryptophyte and eukaryotic phytoplankton numbers, and high molecular weight sugars and Chromophoric Dissolved Organic Matter (CDOM), suggest an organic source. This work points to a significant ocean source of MeSH, highlighting the need for further studies into the distribution and fate of MeSH, and suggests links between atmospheric acetone levels and biogeochemistry over the mid-latitude ocean.

In addition, an intercalibration of DMS<sub>a</sub> at ambient levels using three independently calibrated instruments showed ~15-25% higher mixing ratios from an Atmospheric Pressure Ionisation-Chemical Ionisation Mass Spectrometer (mesoCIMS) compared to a Gas Chromatograph with Sulfur Chemiluminescence Detector (GC-SCD) and proton transfer reaction mass spectrometer (PTR-MS). Some differences were attributed to the DMS<sub>a</sub> gradient above the sea surface and differing approaches of integrated versus discrete measurements. Remaining discrepancies were likely due to different calibration scales, suggesting that further investigation of the stability and/or absolute calibration of DMS standards used at sea is warranted.

## 1 **1 Introduction**

2 Volatile organic compounds (VOCs) are ubiquitous in the atmosphere and have a central role in processes  
3 affecting air quality and climate, via their role in formation of secondary organic aerosol and tropospheric ozone.  
4 The role of the ocean in the global cycle of several VOCs is becoming increasingly recognised, with recent studies  
5 showing that the ocean serves as a major source, sink, or both for many pervasive and climate-active VOCs (Law  
6 et al., 2013; Liss and Johnson, 2014; Carpenter and Nightingale, 2015).

7  
8 The ocean is a major source of reduced volatile sulfur gases and the most well-studied of these is dimethyl sulfide  
9 (DMS) ( $\text{CH}_3\text{SCH}_3$ ), with a global ocean source of  $\sim 28 \text{ Tg S a}^{-1}$  (Lee and Brimblecombe, 2016). Since the  
10 publication of the CLAW hypothesis (Charlson et al., 1987), which proposed a climate feedback loop between  
11 ocean DMS concentrations and cloud droplet concentrations and albedo, extensive investigations have been  
12 undertaken into DMS formation and destruction pathways, ocean-atmosphere transfer, and atmospheric  
13 transformation and impacts on chemistry and climate (Law et al., 2013; Liss and Johnson, 2014; Carpenter et al.,  
14 2012; Quinn and Bates, 2011). Methanethiol or methyl mercaptan (MeSH) ( $\text{CH}_3\text{SH}$ ) is another reduced volatile  
15 organic sulfur gas which originates in the ocean, with a global ocean source estimated to be  $\sim 17\%$  of the DMS  
16 source (Lee and Brimblecombe, 2016). The MeSH ocean source is twice as large as the total of all anthropogenic  
17 sources (Lee and Brimblecombe, 2016). However, the importance of ocean derived MeSH as a source of sulfur  
18 to the atmosphere, and the impact of MeSH and its oxidation products on atmospheric chemistry and climate has  
19 been little-studied.

20 DMS and MeSH in seawater ( $\text{DMS}_{\text{sw}}$  and  $\text{MeSH}_{\text{sw}}$ ) are both produced from precursor dimethylsulfoniopropionate  
21 (DMSP), which is biosynthesised by different taxa of phytoplankton and released into seawater as a result of  
22 aging, grazing, or viral attack (Yoch, 2002). DMSP is then degraded by bacterial catabolism (enzyme catalysed  
23 reaction) via competing pathways that produce either DMS or MeSH (Yoch, 2002). Recent research showed that  
24 bacterium *Pelagibacter* can simultaneously catabolise both  $\text{DMS}_{\text{sw}}$  and  $\text{MeSH}_{\text{sw}}$  (Sun et al., 2016), although it is  
25 not known how widespread this phenomenon is. DMS may also be produced by phytoplankton that directly cleave  
26 DMSP into DMS (Alcolombri et al., 2015). Once released,  $\text{MeSH}_{\text{sw}}$  and  $\text{DMS}_{\text{sw}}$  undergo further reaction in  
27 seawater. These compounds may be assimilated by bacteria, converted to dissolved non-volatile sulfur, be  
28 photochemically destroyed, or in the case of  $\text{MeSH}_{\text{sw}}$ , react with dissolved organic matter (DOM) (Kiene and  
29 Linn, 2000; Kiene et al., 2000; Flöck and Andreae, 1996).  $\text{MeSH}_{\text{sw}}$  has a much higher loss rate constant than  
30  $\text{DMS}_{\text{sw}}$ , with a lifetime on the order of minutes to an hour, compared to  $\sim$  days for  $\text{DMS}_{\text{sw}}$  (Kiene, 1996; Kiene  
31 and Linn, 2000). A fraction ( $\sim 10\%$ ) of  $\text{DMS}_{\text{sw}}$  ventilates to the atmosphere where it can influence particle numbers  
32 and properties through its oxidation products (Simó and Pedrós-Alió, 1999; Malin, 1997). The fraction of  $\text{MeSH}_{\text{sw}}$   
33 ventilating to the atmosphere is poorly constrained.

34  
35 While  $\text{DMS}_{\text{sw}}$  measurements are relatively widespread, only a few studies have measured  $\text{MeSH}_{\text{sw}}$ . During an  
36 Atlantic Meridional Transect cruise in 1998 (Kettle et al., 2001)  $\text{MeSH}_{\text{sw}}$  was higher in coastal and upwelling  
37 regions with the ratio of  $\text{DMS}_{\text{sw}}$  to  $\text{MeSH}_{\text{sw}}$  varying from unity to 30. Leck et al (1991) also reported ratios of  
38  $\text{DMS}_{\text{sw}}/\text{MeSH}_{\text{sw}}$  of 16, 20 and 6 in the Baltic, Kattegat/Skagerrak and North Seas respectively. The drivers of this  
39 variability are unknown, but likely due to variation in the dominant bacterial pathway and/or spatial differences  
40 in degradation processes. More recent  $\text{MeSH}_{\text{sw}}$  measurements in the subarctic NE Pacific Ocean showed the ratio

1 of  $\text{DMS}_{\text{sw}}/\text{MeSH}_{\text{sw}}$  varied from 2-5 indicating that  $\text{MeSH}_{\text{sw}}$  was a significant contributor to the volatile sulfur pool  
2 in this region (Kiene et al., 2017).  $\text{MeSH}_{\text{sw}}$  measurements from these three studies (Kettle et al., 2001; Leck and  
3 Rodhe, 1991; Kiene et al., 2017) were also used to calculate the ocean-atmosphere flux of MeSH, assuming control  
4 from the water side. The flux of  $\text{MeSH}/(\text{MeSH}+\text{DMS})$  ranged from 4-5% in the Baltic and Kattegat sea and 11%  
5 in the North Sea (Leck and Rodhe, 1991), 16% over the North/South Atlantic transect (Kettle et al., 2001), and  
6 ~15% over the North East Sub-arctic Pacific (Kiene et al., 2017). In a review of global organosulfide fluxes, Lee  
7 and Brimblecombe (2016) estimated that ocean sources provide over half of the total global flux of MeSH to the  
8 atmosphere, with a total  $4.7 \text{ Tg S a}^{-1}$ , however this estimate is based on a voyage-average value from a single  
9 study in the North and South Atlantic (Kettle et al., 2001) in which flux measurements varied by several orders  
10 of magnitude.

11  
12 There are very few published atmospheric measurements of  $\text{MeSH}_a$  over the ocean. To the best of our knowledge,  
13 the only prior  $\text{MeSH}_a$  measurements over the ocean were made in 1986 over the Drake Passage and the coastal  
14 and inshore waters west of the Antarctic Peninsula (Berresheim, 1987).  $\text{MeSH}_a$  was detected occasionally at up  
15 to 3.6 ppt, which was roughly 3% of the measured atmospheric  $\text{DMS}_a$  levels (Berresheim, 1987).

16  
17 Once  $\text{MeSH}_{\text{sw}}$  is transferred from ocean to atmosphere ( $\text{MeSH}_a$ ), the main loss pathway for  $\text{MeSH}_a$  is via reaction  
18 with OH and  $\text{NO}_3$  radicals.  $\text{MeSH}_a$  reacts with OH at a rate 2-3 times faster than DMS, and as such  $\text{MeSH}_a$  has  
19 an atmospheric lifetime of only a few hours (Lee and Brimblecombe, 2016). The oxidation pathways and products  
20 that result from  $\text{MeSH}_a$  degradation are still highly uncertain (Lee and Brimblecombe, 2016; Tyndall and  
21 Ravishankara, 1991), though may be somewhat similar to DMS (Lee and Brimblecombe, 2016). This leads to  
22 uncertainty around the final atmospheric fate of the sulfur emitted via MeSH and also the overall impact of  $\text{MeSH}_a$   
23 oxidation on atmospheric chemistry, particularly in regions when MeSH is a significant proportion of total sulfur  
24 emitted.

25 In the case of acetone, positive fluxes from the ocean have been observed in biologically productive areas (Taddei  
26 et al., 2009) and over some subtropical ocean regions (Beale et al., 2013; Yang et al., 2014a; Tanimoto et al.,  
27 2014; Schlundt et al., 2017), however in other subtropical regions, and generally in oligotrophic waters and at  
28 higher latitudes, net fluxes are zero (e.g. ocean and atmosphere in equilibrium), or negative (transfer of acetone  
29 into ocean) (Yang et al., 2014a; Marandino et al., 2005; Beale et al., 2015; Yang et al., 2014b; Schlundt et al.,  
30 2017). Atmospheric acetone ( $\text{acetone}_a$ ) also has significant terrestrial sources including direct biogenic emissions  
31 from vegetation, oxidation of anthropogenic and biogenic hydrocarbons, (predominantly alkanes) and biomass  
32 burning (Fischer et al., 2012). In the ocean,  $\text{acetone}_{\text{sw}}$  is produced photochemically from Chromophoric Dissolved  
33 Organic Matter (CDOM), either directly by direct photolysis or via photosensitizer reactions (Zhou and Mopper,  
34 1997; Dixon et al., 2013; de Bruyn et al., 2012; Kieber et al., 1990). There is also evidence of direct biological  
35 production by marine bacteria (Nemecek-Marshall et al., 1995) and phytoplankton (Schlundt et al., 2017; Sinha  
36 et al., 2007; Halsey et al., 2017). Furthermore,  $\text{acetone}_{\text{sw}}$  has been found to decrease with depth (Beale et al., 2015;  
37 Yang et al., 2014a; Beale et al., 2013; Williams et al., 2004), pointing to the importance of photochemistry and/or  
38 biological activity as the source. Studies have shown  $\text{acetone}_{\text{sw}}$  production linked to photosynthetically active  
39 radiation (PAR) and net shortwave radiation (Sinha et al., 2007; Beale et al., 2015; Zhou and Mopper, 1997), and  
40 Beale et al (2015) found higher  $\text{acetone}_{\text{sw}}$  concentrations in spring and summer compared to autumn and winter.

1 Removal processes include uptake of acetone by bacteria as a carbon source (Beale et al., 2013; Halsey et al.,  
2 2017; Beale et al., 2015; Dixon et al., 2013), gas transfer into the atmosphere, vertical mixing into the deep ocean,  
3 and photochemical destruction (Carpenter and Nightingale, 2015).

4 There are relatively few observations of acetone<sub>sw</sub> and acetone<sub>a</sub> over the remote ocean, particularly in mid and  
5 high latitude regions. An understanding of the spatial distribution of acetone is particularly important due to the  
6 high degree of regional variation in the direction and magnitude of the acetone flux.

7  
8 The Surface Ocean Aerosol Production (SOAP) voyage investigated the relationship between ocean  
9 biogeochemistry and aerosol and cloud processes in a biologically productive but under sampled region in the  
10 remote South West Pacific Ocean (Law et al., 2017). In this work, we present measurements of DMS<sub>a</sub>, MeSH<sub>a</sub>  
11 and acetone<sub>a</sub>, including the largest observed mixing ratios of MeSH<sub>a</sub> in the marine boundary layer to date. We  
12 explore the relationship between DMS<sub>a</sub>, MeSH<sub>a</sub> and acetone<sub>a</sub> as well as the relationship with ocean  
13 biogeochemical parameters. In particular, we investigate links between MeSH<sub>a</sub> and its precursor DMSP for the  
14 first time. We explore whether variability in acetone<sub>a</sub> is linked to biogeochemistry, including warmer subtropical  
15 water and organic precursors such as CDOM as has been reported elsewhere.

16 Given the large uncertainty in the oceanic budget of MeSH, we estimate the importance of MeSH as a source of  
17 atmospheric sulfur in this region and compare with other studies. Finally, we present results from a DMS<sub>a</sub> method  
18 comparison which was undertaken at sea between three independently calibrated measurement techniques.

## 19 **2 Method**

### 20 **2.1 Voyage**

21 The Surface Ocean Aerosol Production (SOAP) voyage took place on the NIWA RV *Tangaroa* over the  
22 biologically productive frontal waters of Chatham Rise (44°S, 174–181°E), east of New Zealand in the South West  
23 Pacific Ocean. The 23 day voyage took place during the austral summer in February – March 2012. The scientific  
24 aim was to investigate interactions between the ocean and atmosphere, and as such the measurement program  
25 included comprehensive characterisation of ocean biogeochemistry, measurement of ocean-atmosphere gas and  
26 particle fluxes and measurement of distribution and composition of trace gases and aerosols in the marine  
27 boundary layer (MBL) (Law et al., 2017). During the voyage, NASA MODIS ocean colour images and underway  
28 sensors were used to identify and map phytoplankton blooms. Three blooms were intensively targeted for  
29 measurement: 1) a dinoflagellate bloom with elevated Chl *a*, DMS<sub>sw</sub> and pCO<sub>2</sub> drawdown and high irradiance  
30 (bloom 1-B1), 2) a coccolithophore bloom (bloom 2 – B2) and 3) a mixed community bloom of coccolithophores,  
31 flagellates and dinoflagellates sampled before (bloom 3a – B3a) and after (bloom 3b – B3b) a storm. For further  
32 voyage and measurement details see Law et al., (2017).

### 33 **2.2 PTR-MS**

34 A high sensitivity proton transfer reaction mass spectrometer (PTR-MS) (Ionicon Analytik) was used to measure  
35 DMS, acetone and methanethiol. The PTR-MS sampled from a 25m 3/8" ID PFA inlet line which drew air from  
36 the crow's nest of the vessel, 28 m above sea level (a.s.l) at 10 L min<sup>-1</sup>. A baseline switch based on relative wind  
37 speed and direction was employed to minimise flow of ship exhaust down the inlet (see Lawson et al., 2015).

1  
2 PTR-MS instrument parameters were as follows: inlet and drift tube temperature of 60°C, a 600V drift tube and  
3 2.2 mbar drift tube pressure ( $E/N=133$  Td). The  $O_2$  signal was < 1% of the primary ion  $H_3O^+$  signal. DMS, acetone  
4 and MeSH were measured at  $m/z$  63, 59 and 49 respectively with a dwell time of 10s. From day of year (DOY)  
5 43 – 49, 19 selected ions including  $m/z$  59 and  $m/z$  63 were measured resulting in 17 mass scans per hour, however  
6 from DOY 49 the PTR-MS measured in scan mode from  $m/z$  21–155, allowing three full mass scans per hour. As  
7 such, MeSH measurements ( $m/z$  49) were made only from DOY 49 onward.

8  
9 VOC-free air was generated using a platinum-coated glass wool catalyst heated to 350°C; 4 times per day this air  
10 was used to measure the background signal resulting from interference ions and outgassing of materials. An  
11 interpolated background signal was used for background correction. Calibrations of DMS and acetone were  
12 carried out daily by diluting calibration gas into VOC – free ambient air (Galbally et al. 2007). Calibration gases  
13 used were a custom ~1 ppm VOC mixture in nitrogen containing DMS and acetone (Scott Specialty gases) and a  
14 custom ~1 ppm VOC calibration mixture in nitrogen containing acetone (Apel Riemer). The calibration gas  
15 accuracy was  $\pm 5\%$ . A calibration gas for MeSH was not available during this voyage. The PTR-MS response to  
16 a given compound is dependent on the chemical ionization reaction rate, defined by the collision rate constant,  
17 and the mass dependent transmission of ions through the mass spectrometer. Given the similarity of the MeSH  
18 and DMS collision rate constant (Williams et al., 1998) and the very similar transmission efficiencies of  $m/z$  63  
19 and  $m/z$  49, we applied the empirically derived PTR-MS response factor for DMS ( $m/z$  63) to the MeSH signal  
20 at  $m/z$  49. The instrument response to DMS and acetone varied by 2% and 5% throughout the voyage respectively.

21  
22 In this work  $m/z$  59 is assumed to be dominated by acetone. Propanal could also contribute to  $m/z$  59, although  
23 studies suggest this is likely low (Beale et al., 2013; Yang et al., 2014a). Similarly,  $m/z$  49 has been attributed to  
24 MeSH, based on a literature review (Feilberg et al., 2010; Sun et al., 2016), and a lack of likely other contributing  
25 species at  $m/z$  49 in the MBL. As such  $m/z$  59 and  $m/z$  49 represent an upper limit for acetone and MeSH  
26 respectively.

27  
28 The minimum detectable limit for a single 10 s measurement of a selected mass was determined using the  
29 principles of ISO 6879 (ISO, 1995). Average detection limits for the entire voyage were as follows:  $m/z$  59  
30 (acetone) 24 ppt,  $m/z$  63 (DMS) 22 ppt,  $m/z$  49 (MeSH) 10 ppt. The percentage of 10 s observations above  
31 detection limits were as follows -  $m/z$  59 100%;  $m/z$  63 98%; and  $m/z$  49 63%. Inlet losses were determined to  
32 be < 2% for isoprene, monoterpenes, methanol and DMS. Acetone and MeSH losses were not determined during  
33 the voyage, however acetone inlet losses were tested previously using ppb level mixture of calibration gases with  
34 PFA inlet tubing and found to be <5%. MeSH has a similar structure and physical properties to DMS at pH < 10  
35 (Sect. 3.2) and so inlet losses are likely to be similar. These small (<5%) losses this could lead to a small  
36 underestimation in reported mixing ratios of  $DMS_a$ ,  $acetone_a$  and  $MeSH_a$ .

## 37 **2.2 DMS Intercomparison**

38 During the SOAP voyage  $DMS_a$  measurements were made using three independently calibrated instruments;  
39 Atmospheric Pressure Ionisation-Chemical Ionisation Mass Spectrometer (mesoCIMS) from the University of

1 California Irvine (UCI), (Bell et al., 2013, 2015), an Ionicon PTR-MS operated by CSIRO (Lawson et al., 2015),  
2 and a HP Gas Chromatograph with Sulfur Chemiluminescence Detector (GC-SCD) operated by NIWA (Walker  
3 et al., 2016).

4  
5 Details of the mesoCIMS and GC-SCD measurement systems are provided by Bell et al. (2015) and Walker et al.  
6 (2016) with a brief description provided here. The mesoCIMS instrument (Bell et al., 2013) ionizes DMS to DMS-  
7 H<sup>+</sup>; m/z=63) by atmospheric pressure proton transfer from H<sub>3</sub>O<sup>+</sup> by passing a heated air stream over a radioactive  
8 nickel foil (Ni-63). The mesoCIMS drew air from the eddy covariance set up on the bow mast at approximately  
9 12m a.s.l. The inlet was a 1/2" ID PFA tube with a total inlet length of 19m and a turbulent flow at 90 standard  
10 litres per minute. The mesoCIMS sub-sampled from the inlet at 1 L m<sup>-1</sup>. A gaseous tri-deuterated DMS standard  
11 (D<sub>3</sub>-DMS) was added to the air sample stream at the entrance to the inlet. The internal standard was ionized and  
12 monitored continuously in the mass spectrometer at m/z=66, and the atmospheric DMS mixing ratio was  
13 computed from the measured 63/66 ratio. The internal standard was delivered from a high pressure aluminium  
14 cylinder and calibrated against a DMS permeation tube prior to and after the cruise (Bell et al., 2015).

15  
16 The GC-SCD system included a semi-automated purge and trap system, a HP 6850 gas chromatograph with  
17 cryogenic preconcentrator/thermal desorber and sulfur chemiluminescence detection (Walker et al 2016). The  
18 system was employed during the voyage for discrete DMS seawater measurements and gradient flux measurement  
19 bag samples (Smith et al., 2018). The system was calibrated using an internal methylethylsulfide (MES)  
20 permeation tube and external DMS permeation tube located in a Dynacalibrator® with a twice daily 5-point  
21 calibration and a running standard every 12 samples (Walker et al., 2016).

22  
23 A DMS measurement intercomparison between the mesoCIMS, GC-SCD and PTR-MS was performed during the  
24 voyage on DOY 64 and DOY 65. Tedlar bags (70 L) with blackout polythene covers were filled with air containing  
25 DMS at sub-ppb levels and were sequentially distributed between all instruments for analysis within a few hours.  
26 On DOY 64, two bags were prepared including ambient air filled from the foredeck and a DMS standard prepared  
27 using a permeation device (Dynacalibrator) and dried compressed air (DMS range 384 – 420 ppt from permeation  
28 uncertainty). On DOY 65, two additional bags were prepared including one ambient air from the foredeck with  
29 tri-deuterated DMS added and a DMS standard prepared using the Dynacalibrator and dried compressed air (DMS  
30 range 331 – 363 ppt). MesoCIMS values are not available for DOY 64 due to pressure differences between bag  
31 and instrument calibration measurements; this was resolved by using an internal standard on DOY 65. For those  
32 analyses, the mesoCIMS and PTR-MS measured DMS at m/z 63 and tri-deuterated DMS at m/z 66, while the  
33 GC-SCD measured both DMS and deuterated DMS as a single peak.

#### 34 **2.4 Biogeochemical measurements in surface waters**

35 Continuous seawater measurements were obtained from surface water sampled by an intake in the vessel's bow  
36 at a depth of ~7m during the SOAP voyage and included underway temperature and salinity (Seabird  
37 thermosalinograph SBE-21), underway chlorophyll *a* (Chl *a*) and backscatter (Wetlabs (Seabird) ECOtriplet),  
38 dissolved DMS (DMS<sub>sw</sub>) (miniCIMS) (Bell et al., 2015). Quenching obscured the Chl *a* signal during daylight  
39 when irradiance > 50 W m<sup>-2</sup>.

1  
2  
3  
4  
5  
6  
7  
8  
9  
  
10  
11  
12  
13  
14  
  
15  
16  
17  
18  
19  
20  
21  
  
22  
23  
24  
25  
26  
27  
28  
29  
30  
31  
32  
33  
34  
35  
36

The following parameters were measured in surface waters (depths 2-10 m) in discrete samples from Niskin bottles on a conductivity – temperature- depth (CTD) rosette: nutrients according to methods described in Law et al., (2011), particulate nitrogen concentration (Nodder et al., 2016), phytoplankton speciation, groups and numbers (optical microscopy of samples preserved in Lugol’s solution) (Safi et al., 2007), Flow cytometry, (Hall and Safi, 2001). In addition, organic parameters measured included High Molecular Weight (HMW) reducing sugars (Somogyi, 1926, 1952; for details see Burrell (2015)), DMSP (Walker et al., 2016) and CDOM measured using a Liquid Waveguide Capillary Cell (Gallet et al., 2013). See Table S1 for measurement specifications and Law et al., (2017) for further details and results for these parameters.

### **3 Results and discussion**

#### **3.1 DMS atmospheric intercalibration**

This section describes a comparison of DMS<sub>a</sub> measurements from bag samples of ambient air and DMS standard mixtures (analysed by GC-SCD, PTR-MS and mesoCIMS, see Section 2), as well as a comparison of ambient DMS<sub>a</sub> measurements (PTR-MS and mesoCIMS).

##### **Comparison of bag samples**

Table 1 summarises the comparison between the GC-SCD, PTR-MS and mesoCIMS instruments for ambient and DMS standard bags prepared and analysed on DOY 64 and 65 (see Section 2.2). The highest DMS levels were measured by the mesoCIMS with GC-SCD and PTR-MS ~20-25 % and ~20-30% lower respectively. The GC-SCD and PTR-MS agreed reasonably well, with a mean difference of 5% (range 0-10%) between instruments for different diluted standard and ambient air bags. There was no clear influence of dry versus humid (ambient) bag samples on the differences between instruments.

##### **Comparison of in situ ambient measurements**

Measurements from the PTR-MS and mesoCIMS were interpolated to a common time stamp for comparison and differences examined only where data were available for both instruments. PTR-MS results for DMS were reported for 10 s every 4 minutes until DOY 49 and then 10 s every 20 minutes until the end of the voyage (Section 2.2). The mesoCIMS measured DMS continuously and reported 10 minute averages. As such the PTR-MS measured only a ‘snapshot’ of the DMS<sub>a</sub> levels in each measurement cycle of 4 or 20 minutes. This was a potential source of difference between the two instruments when DMS levels changed rapidly (Bell et al., 2015).

The mesoCIMS was deployed primarily for DMS eddy covariance measurements, while the PTR-MS was deployed to measure atmospheric mixing ratios of a range of VOCs. As such, the mesoCIMS was situated on the foredeck and sampled from the eddy covariance set up on the bow mast (12m a.s.l), while the PTR-MS was sited further back in the vessel and sampled from the crows nest (28m a.s.l). Therefore, due to different intake heights, a further source of the difference between the PTR-MS and mesoCIMS measurements is likely due to vertical gradients in DMS caused by turbulent mixing of the local surface DMS flux into the atmospheric surface layer. On days with a strong DMS source and/or more stable stratification in the boundary layer, a significant decrease

1 with height is expected (Smith et al., 2018). If all the DMS observed was due to local emissions, the vertical  
2 gradient would be described by Equation 2 from Smith et al (2018):

$$F \equiv -u^* C^* = -\frac{u^* k}{\varphi c(z/L)} \left( \frac{\partial c}{\partial \ln z} \right) \quad (1)$$

3  
4  
5  
6 Where  $u^*$  is friction velocity,  $C^*$  is scaling parameter for gas concentration,  $k$  is the von Kármán constant,  $\varphi c$  is  
7 the stability function for mass,  $z$  is the height above mean water level and  $L$  is the Monin-Obukhov scaling length  
8 representing atmospheric stability. Atmospheric stability is a measure of the degree of vertical motion in the  
9 atmosphere, where  $z/L = 0$  indicates neutral stability,  $z/L > 0$  indicates a stable atmosphere and  $z/L < 0$  indicates  
10 an unstable atmosphere.

11 Figure 1 shows wind speed, absolute wind direction and atmospheric stability, DMS<sub>a</sub> levels from the voyage  
12 measured by PTR-MS and mesoCIMS, relative percent difference between the two measurements (normalised to  
13 the mesoCIMS), and observed absolute difference in DMS<sub>a</sub> between the two measurements, as well as the  
14 expected calculated difference (Eq 1) between two measurements due to the DMS<sub>a</sub> concentration gradient.

15 The mesoCIMS and PTR-MS DMS<sub>a</sub> data showed similar temporal behaviour over the voyage (Fig. 1). From DOY  
16 44 – 46 there was an average of 50% ( $\pm 10\%$ ) relative difference between measurements, yet on DOY 47 this  
17 difference decreased suddenly to an average of  $\sim 20\%$  ( $\pm 20\%$ ).

18 Overall, agreement between instruments improved with time during the voyage, with differences of several  
19 hundred ppt of DMS observed in the first few days decreasing to differences of only 10-20 ppt by the end of the  
20 voyage. The agreement between instruments improves with increasing wind speeds (Fig. 1). The expected  
21 calculated difference between DMS<sub>a</sub> at the two inlet heights due to the DMS concentration gradient also decreases  
22 throughout the voyage. This indicates that the increasing agreement between instruments during the voyage was  
23 likely influenced by a progressively well mixed atmosphere leading to weaker DMS vertical gradients.

24 The reason for the improved agreement between mesoCIMS and PTR-MS at DOY 47 is unlikely due to a decrease  
25 in the DMS concentration gradient (Fig. 1 bottom panel), but is more likely due to changes in instrument  
26 calibration or other differences. However careful inspection of the instrument parameters, configurations and  
27 calibration responses prior to DOY 47 did not identify the cause of the disagreement.

28 Figure 2a shows paired DMS<sub>a</sub> data from the mesoCIMS versus PTR-MS over the whole voyage and Fig 2b shows  
29 paired mesoCIMS data versus PTR-MS data converted to same height as the mesoCIMS with the expected DMS  
30 difference calculated from the eddy covariance estimate of DMS flux (from mesoCIMS) and eddy diffusivity  
31 (PTR-MS DMS<sub>a</sub> + calculated difference between the two intake heights). The reduced major axis regression  
32 relationship between the two measurements systems for uncorrected data gives a slope of  $0.74 \pm 0.02$ , while for  
33 the corrected data gives  $0.81 \pm 0.02$  ( $r^2 = 0.69$ ). The gradient-corrected slope agrees with the ambient bag sample  
34 ratio from the method comparison (PTR-MS / mesoCIMS =  $0.81 \pm 0.16$ ) (Table 1). Correcting for the DMS  
35 gradient improved the comparison between PTR-MS and mesoCIMS. The remaining  $\sim 20\%$  difference is likely  
36 due to instrument calibration differences and differing approaches of integrated versus discrete measurements.

37  
38 There was no obvious impact of absolute wind direction on the differences observed between measurement  
39 systems. Note that due to the Baseline switch which was employed to avoid sampling ship exhaust down the PTR-



1 MS inlet (Lawson et al., 2015) the PTR-MS did not sample during certain relative wind directions. However, this  
2 does not affect the comparison which was undertaken only when data were available for both instruments.

### 3 **3.2 Ambient atmospheric data**

4 Atmospheric mixing ratios of MeSH<sub>a</sub>, DMS<sub>a</sub> and acetone<sub>a</sub> are shown along the voyage track in Fig. 3 with bloom  
5 locations highlighted. Figure 4 shows a time series of MeSH<sub>a</sub>, DMS<sub>a</sub>, acetone<sub>a</sub>, MeSH<sub>a</sub>/DMS<sub>a</sub> (all measured with  
6 PTR-MS) as well as DMS<sub>sw</sub> (miniCIMS) from Bell et al (2015), Chl<sub>a</sub>, irradiance, wind speed, wind direction and  
7 sea and air temperature. Note that MeSH<sub>a</sub> measurements started on DOY 49, the last day of bloom B1. The fraction  
8 of back trajectories arriving at the ship that had been in contact with land masses in the previous 10 days is also  
9 shown with a value of 0 indicating no contact with land masses in the preceding 10 days. This was calculated  
10 using the Lagrangian Numerical Atmospheric-dispersion Modelling Environment (NAME) for the lower  
11 atmosphere (0–100 m) as time-integrated particle density (g s m<sup>-3</sup>), every 3 hours from ship location (Jones et al,  
12 2007) as shown in Law et al. (2017). Where air contacted land masses this was the New Zealand land mass in  
13 almost all cases.

14 MeSH<sub>a</sub> ranged from below detection limit (< 10 ppt) to 65 ppt, DMS<sub>a</sub> ranged from below detection limit (~22 ppt)  
15 up to 957 ppt, and acetone<sub>a</sub> ranged from 50–1500 ppt (Table 2). The ratio of MeSH<sub>a</sub> to DMS<sub>a</sub> ranged from 0.03 -  
16 0.36 (mean 0.14) for measurements when both were above the minimum detectable limit. Periods of elevated  
17 DMS<sub>a</sub> generally correspond to periods of elevated DMS<sub>sw</sub>. Both DMS<sub>a</sub> and DMS<sub>sw</sub> were very high during B1,  
18 during the transect to B2, and the first half of B2 occupation. MeSH<sub>a</sub> variability broadly correlates with DMS<sub>a</sub>  
19 and DMS<sub>sw</sub>, with highest levels during B2 (no data available for B1). The highest acetone<sub>a</sub> levels observed occur  
20 during B2, and a broad acetone peak during B1 of 700 ppt (~DOY 49) overlaps with but is slightly offset from  
21 the largest DMS<sub>a</sub> peak during the voyage (~957 ppt). DMS<sub>a</sub>, acetone<sub>a</sub> and MeSH<sub>a</sub> were somewhat lower during  
22 B3a and lowest during the B3b, the post-storm part of that bloom B3 (see Law et al., 2017). In general, DMS<sub>a</sub>  
23 levels during B1 were at the upper range of those found in prior studies elsewhere (Lana et al., 2011; Law et al.,  
24 2017). MeSH<sub>a</sub> levels during B2 ranged from below detection limit (~10 ppt) up to 65 ppt (mean 25 ppt), which  
25 is substantially higher than the only comparable measurements from the Drake Passage and the coastal and inshore  
26 waters west of the Antarctic Peninsula (3.6 ppt) (Berresheim, 1987). The average acetone<sub>a</sub> levels during this study  
27 were broadly comparable to those from similar latitudes reported in the South Atlantic and Southern Ocean  
28 (Williams et al., 2010) and at Cape Grim (Galbally et al., 2007). Acetone<sub>a</sub> during SOAP was generally lower than  
29 at similar latitudes at Mace Head (Lewis et al., 2005), the Southern Indian Ocean (Colombet et al., 2009) and also  
30 the marine subtropics (Read et al., 2012; Schlundt et al., 2017; Warneke and de Gouw, 2001; Williams et al., 2004).

31  
32 There were two occasions when elevated acetone<sub>a</sub> corresponded closely to increased land influence – during B1  
33 on DOY 48–49 (maximum land influence 12%) and DOY 60 (maximum land influence 20%) (Fig 4). Both these  
34 periods corresponded to winds from the north, and back trajectories show that the land mass contacted was the  
35 southern tip of New Zealand's North Island (including the city of Wellington and the northern section of the South  
36 Island in both cases). The acetone measured during these periods may have been emitted from anthropogenic and  
37 biogenic sources and from photochemical oxidation of hydrocarbon precursors (Fischer et al., 2012). The acetone  
38 enhancement relative to the degree of land influence was higher on DOY 48–49 than DOY 60 possibly due to  
39 different degrees of dilution of the terrestrial plume, or different terrestrial source strengths.

1 The period with the highest acetone levels during B2 (1508 ppt) corresponds with a period of negligible land  
2 influence (0.3%) indicating a non-terrestrial, possibly local source of acetone<sub>a</sub>. Neither MeSH<sub>a</sub> or DMS<sub>a</sub> maxima  
3 corresponded with peaks in land influence, except for the latter part of the DMS<sub>a</sub> maximum on DOY 48-49;  
4 however the source of DMS<sub>a</sub> during DOY 48 – 49 is attributed to local ocean emissions as shown by strong  
5 association between DMS<sub>sw</sub> and DMS<sub>a</sub> during this period (Fig. 4).

6  
7 Correlations of DMS<sub>a</sub>, MeSH<sub>a</sub> and acetone<sub>a</sub> were examined to identify possible common marine sources or  
8 processes influencing atmospheric levels (Table 3). Only data above minimum detectable limit were included in  
9 the regressions. Acetone<sub>a</sub> data likely influenced by terrestrial sources (DOY 48-49 and 60, described above) were  
10 removed from this analysis. A moderate correlation ( $R^2=0.5$ ,  $p<0.0001$ ) was found between DMS<sub>a</sub> and MeSH<sub>a</sub>  
11 during B2 with a correlation of  $R^2=0.3$ , ( $p<0.0001$ ) between DMS<sub>a</sub> and MeSH<sub>a</sub> for all data (Fig. 5). During B2 the  
12 slope was 0.13 (MeSH<sub>a</sub> roughly 13% of the DMS<sub>a</sub> mixing ratios), while for all data the slope was 0.07 (including  
13 blooms and transiting between blooms).

14  
15 MeSH<sub>sw</sub> and DMS<sub>sw</sub> are produced from bacterial catabolism of DMSP via two competing processes, so the amount  
16 of DMS<sub>sw</sub> vs MeSH<sub>sw</sub> produced from DMSP will depend on the relative importance of these two pathways at any  
17 given time. Additional sources of DMS<sub>sw</sub>, such as phytoplankton that cleave DMSP into DMS will also influence  
18 the amount of DMS<sub>sw</sub> vs MeSH<sub>sw</sub> produced. A phytoplankton-mediated source of DMS<sub>sw</sub> was likely to be an  
19 important contributor to the DMS<sub>sw</sub> pool during the SOAP voyage, either through indirect processes (zooplankton  
20 grazing, viral lysis and senescence) or direct processes (algal DMSP-lyase activity) (Lizotte et al., 2017). The  
21 relative loss rates of DMS<sub>sw</sub> and MeSH<sub>sw</sub> through oxidation, bacterial uptake or reaction with DOM will also  
22 influence the amount of each gas available to transfer to the atmosphere, with MeSH<sub>sw</sub> having a much faster loss  
23 rate in sea water than DMS<sub>sw</sub> (Kiene and Linn, 2000; Kiene et al., 2000). Differences between the gas transfer  
24 velocities of DMS and MeSH would also affect the atmospheric mixing ratios. Such differences are likely to be  
25 small, due to similar solubilities (Sander, 2015) and diffusivities (Johnson, 2010). A final factor that will influence  
26 the slope of DMS<sub>a</sub> vs MeSH<sub>a</sub> is the atmospheric lifetime (Table 2). The average lifetimes of DMS<sub>a</sub> and MeSH<sub>a</sub> in  
27 this study are estimated at 24 and 9 hours respectively with respect to OH, calculated using DMS reaction rate of  
28 OH from Berresheim et al. (1987), the MeSH reaction rate from Atkinson et al. (1997) and OH concentration  
29 calculated as described in Lawson et al. (2015). Hence, the correlation between DMS<sub>a</sub> and MeSH<sub>a</sub> reflects the  
30 common seawater source of both gases, while the differing slopes between B2 and all data probably reflect the  
31 different sources and atmospheric lifetimes. While a correlation between MeSH and DMS has been observed in  
32 sea water samples previously (Kettle et al., 2001; Kiene et al., 2017), to our knowledge this is the first time that a  
33 correlation between MeSH<sub>a</sub> and DMS<sub>a</sub> has been observed in the atmosphere over the remote ocean.

34 There were several weak ( $R^2 \leq 0.2$ ) but significant correlations between DMS<sub>a</sub> and acetone<sub>a</sub>, and acetone<sub>a</sub> and  
35 MeSH<sub>a</sub> (Table 3). The correlation of acetone<sub>a</sub> with DMS<sub>a</sub> may reflect elevated organic sources for photochemical  
36 production of acetone in regions of high dissolved sulfur species. A further discussion of drivers of DMS<sub>a</sub>, acetone<sub>a</sub>  
37 and MeSH<sub>a</sub> mixing ratios is provided in Section 3.3.

38 An additional factor which may influence the measured mixing ratios of DMS<sub>a</sub>, MeSH<sub>a</sub> and acetone<sub>a</sub> is  
39 entrainment of air from the free troposphere into the MBL. For short-lived DMS and MeSH (Table 2), free  
40 tropospheric air is most likely to be depleted in these gases compared to air sampled close to the ocean surface.

1 Acetone is relatively long lived (Table 2) and has significant terrestrial sources (Fischer et al., 2012), and so  
 2 depending on the origin of the free tropospheric air, could be enhanced or depleted relative to MBL air. Figure 6  
 3 shows the voyage-average diurnal cycles for DMS<sub>a</sub>, MeSH<sub>a</sub> and acetone<sub>a</sub>. The diurnal cycle of DMS<sub>a</sub> shows  
 4 variations by almost a factor of 3 from morning (maximum at 8:00 hrs ~ 330 ppt) to late afternoon (minimum,  
 5 16:00 hrs ~ 120 ppt). A DMS<sub>a</sub> diurnal cycle with sunrise maximum and late afternoon minimum has been  
 6 observed in many previous studies and is attributed to photochemical destruction by OH. This includes Cape Grim  
 7 baseline station which samples air from the Southern Ocean (average minimum and maximum ~40-70 ppt) (Ayers  
 8 and Gillett, 2000), over the tropical Indian ocean (average minimum and maximum ~25-60 ppt (Warneke and de  
 9 Gouw, 2001) and at Kiritimati in the tropical Pacific (average minimum and maximum 120-200 ppt) (Bandy et al,  
 10 1996). The higher atmospheric levels in this study are due to high DMS<sub>sw</sub> concentrations (>15 nM). The amplitude  
 11 of the DMS diurnal cycle is likely to have been influenced by stationing the vessel over blooms with high DMS<sub>sw</sub>  
 12 from 8:00 hrs each day and regional mapping of areas with lower DMS<sub>sw</sub> overnight (Law et al., 2017).

13  
 14 The diurnal cycle for MeSH<sub>a</sub> (Fig. 6 b) shows similar behaviour to DMS<sub>a</sub> with the mixing ratios varying by a  
 15 factor of ~2 with the minimum mixing ratio occurring at around 16:00 hrs (the same time as minimum DMS<sub>a</sub>).  
 16 The most important sink of MeSH<sub>a</sub> is thought to be oxidation by OH (Lee and Brimblecombe, 2016), and the  
 17 minima in late afternoon may be due to destruction by OH. The decoupling of the DMS and MeSH diurnal cycles  
 18 between 4:00 – 8:00 hrs, with DMS increasing and MeSH decreasing, is likely due to the differing production  
 19 pathways as well as the possibility of additional sinks for MeSH in the ocean during this time. This period may  
 20 also have been influenced by mapping areas with lower DMS<sub>sw</sub> overnight and stationing the vessel over blooms  
 21 with high DMS<sub>sw</sub> from 8:00 hrs each day, as described above.

22 The acetone<sub>a</sub> diurnal cycle (Fig. 6c) with land-influenced data removed shows reasonably consistent mixing ratios  
 23 from the early morning until midday, with an overall increase in acetone levels during the afternoon hours from  
 24 14:00 hrs onwards, then decreasing again at night, which is the opposite to the behaviour of DMS<sub>a</sub> and MeSH<sub>a</sub>.  
 25 Acetone is long lived (~60 days – Table 2) with respect to oxidation by OH. The increase of acetone<sub>a</sub> mixing  
 26 ratios in the afternoon may indicate photochemical production from atmosphere or sea surface precursors but there  
 27 was no correlation between irradiance and acetone<sub>a</sub> during the voyage.

28

### 29 3.3 Flux calculation from nocturnal accumulation of MeSH

30 MeSH and DMS fluxes ( $F$ ) were calculated according to the nocturnal accumulation method (Marandino et al,  
 31 2007). This approach assumes that nighttime photochemical losses are negligible, and that sea surface emissions  
 32 accumulate overnight within the well-mixed marine boundary layer (MBL). Horizontal homogeneity and zero  
 33 flux at the top of the boundary layer are also assumed. The air-sea flux is calculated from the increase in MeSH  
 34 and DMS. For example:

35

$$36 \quad F = \frac{\partial[\text{MeSH}]}{\partial t} \times h \quad (2)$$

37

38 where [MeSH] is the concentration of MeSH in mol m<sup>-3</sup> and  $h$  = average nocturnal MBL for the voyage of 1135  
 39 m ± 657 m, estimated from nightly radiosonde flights.

1 DMS and MeSH fluxes were calculated for 3 nights (DOY 52, 54 and 60) (Table 4) when linear increases in  
2 mixing ratios occurred over several hours (Fig 4). The MeSH flux was lowest on DOY 52 prior to B2 ( $3.5 \pm 2$   
3  $\mu\text{mol}^{-1} \text{m}^{-2} \text{day}^{-1}$ ), higher on DOY 60 during B3a ( $4.8 \pm 2.8 \mu\text{mol}^{-1} \text{m}^{-2} \text{day}^{-1}$ ), and highest on DOY 42 during B2  
4 ( $5.8 \pm 3.4 \mu\text{mol}^{-1} \text{m}^{-2} \text{day}^{-1}$ ). There are no MeSH measurements during B1. The percentage of  
5 MeSH/(DMS+MeSH) emitted varied from 14% for DOY 60 (B3a), up to 23% and 24% for DOY 54 (B2) and  
6 DOY 52 (prior to B2).

7 For comparison the DMS fluxes measured using eddy covariance (EC) at the same time are given in Table 4 (Bell  
8 et al., 2015). DMS fluxes calculated using the nocturnal accumulation method are within the variability of the EC  
9 fluxes (Bell et al., 2015).

10 The average MeSH flux calculated from this study ( $4.7 \mu\text{mol} \text{m}^{-2} \text{day}^{-1}$ ) was more than 4 times higher than average  
11 MeSH fluxes from previous studies in the North/South Atlantic (Kettle et al., 2001) and in the Baltic, Kattegat  
12 and North Sea (Leck and Rodhe, 1991) (Table 5). The MeSH fluxes calculated from this work are comparable to  
13 maximum values reported by Kettle et al., (2001) which were observed in localised coastal and upwelling regions.  
14 The average emission of MeSH compared to DMS (MeSH/(DMS+MeSH)) was higher in this study (20%) than  
15 previous studies (Table 5) including the Baltic, Kattegat and North Sea (5%, 4% and 11%), North/South Atlantic  
16 (16%), and a recent study from the Northeast Sub-arctic Pacific (~15%) (Kiene et al., 2017). Note that other  
17 sulfur species such as dimethyl disulphide (DMDS), carbon disulphide ( $\text{CS}_2$ ) and hydrogen sulphide ( $\text{H}_2\text{S}$ )  
18 typically make a very small contribution to the total sulfur compared to DMS and MeSH (Leck and Rodhe,  
19 1991; Kettle et al., 2001; Yvon et al., 1993) and so are neglected from this calculation.

### 20 **3.4 Correlation with ocean biogeochemistry**

21 To investigate the influence of biogeochemical parameters on atmospheric mixing ratios of  $\text{MeSH}_a$ ,  $\text{DMS}_a$  and  
22 acetone<sub>a</sub>, Spearman rank correlations were undertaken to identify relationships significant at the 95% confidence  
23 interval (CI). Table 6 summarises the correlation coefficients and p values for significant correlations.  $\text{MeSH}_a$ ,  
24  $\text{DMS}_a$  and acetone<sub>a</sub> data were averaged one hour either side of the CTD water entry time for the analysis.

25  
26 Sulfur gases  $\text{MeSH}_a$  and  $\text{DMS}_a$  are short lived and so the air-sea flux is controlled by the seawater concentration.  
27 By contrast, acetone<sub>a</sub> is much longer lived in the atmosphere (~60 days), so the air/sea gradient can be influenced  
28 by both oceanic emissions and atmospheric transport from other sources. As such, the variability in acetone<sub>a</sub>  
29 mixing ratios may be driven by ocean/air exchange and/or input of acetone<sub>a</sub> to the boundary layer from terrestrial  
30 sources, the upper atmosphere, or in situ production. This means that correlation analyses to explore ocean  
31 biogeochemical sources of acetone<sub>a</sub> may be confounded by atmospheric sources. Removal of land influenced  
32 data reduces the likelihood of this but observed increases in atmospheric acetone could still be from in situ  
33 processes such as oxidation of organic aerosol or mixing from above the boundary layer.

34  
35 Both  $\text{MeSH}_a$  and  $\text{DMS}_a$  have a strong positive and highly significant relationship with  $\text{DMS}_{\text{sw}}$ , and a moderate  
36 correlation with discrete measurements of  $\text{DMSP}_t$  (total) and  $\text{DMSP}_p$  (particulate). The correlation of  $\text{DMS}_a$  with  
37  $\text{DMS}_{\text{sw}}$  can be attributed to the positive flux of DMS out of the ocean, however the correlation of  $\text{MeSH}_a$  with  
38  $\text{DMS}_{\text{sw}}$  is likely due to a common ocean precursor of both gases (DMSP) albeit via different production pathways.  
39  $\text{DMS}_a$  and  $\text{MeSH}_a$  correlate with  $\text{DMSP}_p$  (particulate) but not with  $\text{DMSP}_d$  (dissolved). For  $\text{DMS}_a$ , the correlation

1 may reflect that a proportion of the DMS observed was derived directly from phytoplankton rather than being  
2 bacterially mediated, in agreement with findings by Lizotte et al., (2017); however, as demethylation of DMSP<sub>a</sub>  
3 represents the primary source of MeSH the lack of correlation is surprising. The latter may reflect MeSH sinks in  
4 surface water associated with organics and particles (Kiene, 1996), and could be confirmed via incubation  
5 experiments. DMS<sub>a</sub> also correlated with particulate nitrogen and showed a moderate negative correlation with  
6 silicate that may reflect lower DMS production in diatom-dominated waters.

7  
8 Acetone<sub>a</sub> shows a positive correlation with temperature and negative correlation with nutrients. This is consistent  
9 with reported sources of acetone<sub>sw</sub> in warmer subtropical waters (Beale et al., 2013; Yang et al., 2014a; Tanimoto  
10 et al., 2014; Schlundt et al., 2017). The positive relationship with organic material including HMW sugars and  
11 CDOM may reflect a photochemical ocean source (Zhou and Mopper, 1997; Dixon et al., 2013; de Bruyn et al.,  
12 2012; Kieber et al., 1990), or possibly a biological source (Nemecek-Marshall et al., 1995; Nemecek-Marshall et  
13 al., 1999; Schlundt et al., 2017; Sinha et al., 2007; Halsey et al., 2017) as indicated by the correlations with  
14 cryptophyte and picoeukaryote abundance. Correlation with particle backscatter suggests potential links between  
15 acetone<sub>a</sub> and coccolithophores (Sinha et al., 2007). Alternatively, the positive correlations of acetone<sub>a</sub> with these  
16 organic components of sea water may reflect acetone production in the atmosphere from photochemical oxidation  
17 of ocean-derived organic aerosols (Pan et al., 2009; Kwan et al., 2006; Jacob et al., 2002). Sea water acetone  
18 measurements would allow further elucidation of the relationships between acetone<sub>a</sub> and biogeochemical  
19 parameters identified in this study. More generally, mesocosm, or laboratory studies could be employed to  
20 identify the explicit sources and production mechanisms of these gases in Chatham Rise waters.

#### 21 **4 Implications and conclusions**

22 Mixing ratios of short-lived MeSH<sub>a</sub> over the remote ocean of up to 65 ppt in this study are the highest observed  
23 to date and provide evidence that MeSH transfers from the ocean into the atmosphere and may be present at non-  
24 negligible levels in the atmosphere over other regions of high biological productivity. The average MeSH flux  
25 calculated from this study ( $4.7 \mu\text{mol m}^{-2} \text{day}^{-1}$ ) was at least 4 times higher than average MeSH fluxes from previous  
26 studies and is comparable to maximum MeSH flux values reported in localised coastal and upwelling regions of  
27 the North/South Atlantic (Kettle et al., 2001) (Table 5). The average emission of MeSH compared to DMS  
28 (MeSH/(DMS+MeSH)) was higher in this study (20%) than previous studies (4-16%), indicating MeSH provides  
29 a significant transfer of sulfur to the atmosphere in this region. Taken together with other studies, the magnitude  
30 of the ocean MeSH flux to the atmosphere appears to be highly variable as is the proportion of S emitted as MeSH  
31 compared to DMS. For example, MeSH fluxes in the Kettle et al. (2001) study varied by orders of magnitude,  
32 and in some cases the MeSH flux equalled the DMS flux. Similarly, DMS<sub>sw</sub>/MeSH<sub>sw</sub> concentration ratios have  
33 varied substantially (Kettle et al., 2001, Leck and Rodhe, 1991 and Kiene et al., 2017). As such, further studies  
34 are needed to investigate the spatial distribution of MeSH both in sea water and the atmosphere as well as the  
35 importance of MeSH as a source of atmospheric sulfur. The fate of atmospheric MeSH sulfur in the atmosphere  
36 is also highly uncertain, in terms of its degradation pathways and reactions, and intermediate and final degradation  
37 products. For example, the impact that oxidation of MeSH<sub>a</sub> has on the oxidative capacity of the MBL and on other  
38 processes such as particle formation or growth to the best of our knowledge remains largely unknown, and further  
39 work is needed on its atmospheric processes and fate.

1 A correlation analysis of MeSH<sub>a</sub> and biogeochemical parameters was undertaken for the first time and showed  
2 that MeSH<sub>a</sub>, as well as DMS<sub>a</sub> correlated with their ocean precursor, DMSP, and also correlated with seawater  
3 DMS (DMS<sub>sw</sub>). The correlation of MeSH<sub>a</sub> with DMS<sub>sw</sub> is likely due to a common ocean precursor of both gases  
4 (DMSP) which are produced via different pathways.

5 Correlation of acetone<sub>a</sub> with biogeochemical parameters suggests a source of acetone from warmer subtropical  
6 ocean waters, in line with other studies, with positive correlations between acetone<sub>a</sub> and ocean temperature, high  
7 molecular weight sugars, cryptophyte and eukaryote phytoplankton, chromophoric dissolved organic matter  
8 (CDOM) and particle backscatter, and a negative correlation with nutrients. While data with a terrestrial source  
9 influence was removed from this analysis, it is still possible that the acetone peaks observed may not have been  
10 due to a positive flux of acetone from the ocean, but rather from in situ processes leading to acetone production  
11 such as oxidation of marine-derived organic aerosol.

12 Finally, the SOAP voyage provided the opportunity to compare 3 independently calibrated DMS<sub>a</sub> measurement  
13 techniques at sea (PTR-MS, mesoCIMS and GC-SCD). Agreement between the three techniques was generally  
14 good, however some systematic differences between the datasets were observed. Some of these differences were  
15 attributed to the near surface DMS gradient and the use of different inlet heights (28 and 12 m a.s.l for the PTR-  
16 MS and mesoCIMS respectively), as well as differing approaches of integrated versus discrete measurements.  
17 The remaining discrepancies are likely due to differences in calibration scales, suggesting that further  
18 investigation of the stability and/or absolute calibration of DMS standards used at sea is warranted.

## 19 **Data availability**

20 DMS, acetone and MeSH data are available via the CSIRO data access portal (DAP) at  
21 <https://doi.org/10.25919/5d914b00c5759>. Further data are available by emailing the corresponding author or the  
22 voyage leader: cliff.law@niwa.co.nz.

## 23 **Author Acknowledgements**

24 We thank the officers and crew of the RV Tangaroa and NIWA Vessels for logistics support. Many thanks to John  
25 McGregor (NIWA) for providing land influence data and to Paul Selleck and Erin Dunne (CSIRO) for helpful  
26 discussions. Thanks to the NIWA Visiting Scientist Scheme and CSIRO's Capability Development Fund for  
27 providing financial support for Sarah Lawson's participation in the SOAP voyage.

## 28 **References**

29  
30 Alcolombri, U., Ben-Dor, S., Feldmesser, E., Levin, Y., Tawfik, D. S., and Vardi, A.: Identification of the algal  
31 dimethyl sulfide-releasing enzyme: A missing link in the marine sulfur cycle, *Science*, 348, 1466-1469,  
32 10.1126/science.aab1586, 2015.  
33 Atkinson, R.: Kinetics and mechanisms of the gas-phase reactions of the hydroxyl radical with organic compounds  
34 under atmospheric conditions, *Chem. Rev.*, 86, 69-201, 10.1021/cr00071a004, 1986.  
35 Atkinson, R., Baulch, D. L., Cox, R. A., Hampson, R. F., Kerr, J. A., Rossi, M. J., and Troe, J.: Evaluated Kinetic,  
36 Photochemical and Heterogeneous Data for Atmospheric Chemistry: Supplement V. IUPAC Subcommittee on  
37 Gas Kinetic Data Evaluation for Atmospheric Chemistry, *Journal of Physical and Chemical Reference Data*, 26,  
38 521-1011, 10.1063/1.556011, 1997.

1 Ayers, G. P., and Gillett, R. W.: DMS and its oxidation products in the remote marine atmosphere: implications  
2 for climate and atmospheric chemistry, *Journal of Sea Research*, 43, 275-286, 2000.

3 Bandy, A. R., Thornton, D. C., Blomquist, B. W., Chen, S., Wade, T. P., Ianni, J. C., Mitchell, G. M., and Nadler,  
4 W.: Chemistry of dimethylsulfide in the equatorial Pacific atmosphere, *Geophysical Research Letters*, 23, 741-  
5 744, 10.1029/96gl00779, 1996.

6 Beale, R., Dixon, J. L., Arnold, S. R., Liss, P. S., and Nightingale, P. D.: Methanol, acetaldehyde, and acetone in  
7 the surface waters of the Atlantic Ocean, *Journal of Geophysical Research: Oceans*, 118, 5412-5425,  
8 10.1002/jgrc.20322, 2013.

9 Beale, R., Dixon, J. L., Smyth, T. J., and Nightingale, P. D.: Annual study of oxygenated volatile organic  
10 compounds in UK shelf waters, *Marine Chemistry*, 171, 96-106, <https://doi.org/10.1016/j.marchem.2015.02.013>,  
11 2015.

12 Bell, T. G., De Bruyn, W., Miller, S. D., Ward, B., Christensen, K. H., and Saltzman, E. S.: Air-sea  
13 dimethylsulfide (DMS) gas transfer in the North Atlantic: evidence for limited interfacial gas exchange at high  
14 wind speed, *Atmos. Chem. Phys.*, 13, 11073-11087, 10.5194/acp-13-11073-2013, 2013.

15 Bell, T. G., De Bruyn, W., Marandino, C. A., Miller, S. D., Law, C. S., Smith, M. J., and Saltzman, E. S.:  
16 Dimethylsulfide gas transfer coefficients from algal blooms in the Southern Ocean, *Atmos. Chem. Phys.*, 15,  
17 1783-1794, 10.5194/acp-15-1783-2015, 2015.

18 Berresheim, H.: Biogenic sulfur emissions from the Subantarctic and Antarctic Oceans, *Journal of Geophysical*  
19 *Research*, 92, 13245-13262, 10.1029/JD092iD11p13245, 1987.

20 Burrell, T. J.: Bacterial extracellular enzyme activity in a future ocean, Ph.D thesis, Victoria University of  
21 Wellington, 324 pp., 2015.

22 Carpenter, L. J., Archer, S. D., and Beale, R.: Ocean-atmosphere trace gas exchange, *Chem. Soc. Rev.*, 41, 6473-  
23 6506, 10.1039/c2cs35121h, 2012.

24 Carpenter, L. J., and Nightingale, P. D.: Chemistry and Release of Gases from the Surface Ocean, *Chem. Rev.*,  
25 115, 10, 4015-4034, 10.1021/cr5007123, 2015.

26 Charlson, R., Lovelock, J., Andreae, M., and Warren, S.: Oceanic phytoplankton, atmospheric sulphur, cloud  
27 albedo and climate., *Nature*, 326, 10.1038/326655a0, 1987.

28 Colomb, A., Gros, V., Alvain, S., Sarda-Estève, R., Bonsang, B., Moulin, C., Klupfel, T., and Williams, J.:  
29 Variation of atmospheric volatile organic compounds over the Southern Indian Ocean (30-49° S), *Environmental*  
30 *Chemistry*, 6, 70-82, 10.1071/en08072, 2009.

31 de Bruyn, W. J., Clark, C. D., Pagel, L., and Takehara, C.: Photochemical production of formaldehyde,  
32 acetaldehyde and acetone from chromophoric dissolved organic matter in coastal waters, *Journal of*  
33 *Photochemistry and Photobiology a-Chemistry*, 226, 16-22, 10.1016/j.jphotochem.2011.10.002, 2012.

34 Dixon, J. L., Beale, R., and Nightingale, P. D.: Production of methanol, acetaldehyde, and acetone in the Atlantic  
35 Ocean, *Geophysical Research Letters*, 40, 4700-4705, 10.1002/grl.50922, 2013.

36 Feilberg, A., Liu, D., Adamsen, A. P. S., Hansen, M. J., and Jonassen, K. E. N.: Odorant Emissions from Intensive  
37 Pig Production Measured by Online Proton-Transfer-Reaction Mass Spectrometry, *Environmental Science &*  
38 *Technology*, 44, 5894-5900, 10.1021/es100483s, 2010.

39 Fischer, E. V., Jacob, D. J., Millet, D. B., Yantosca, R. M., and Mao, J.: The role of the ocean in the global  
40 atmospheric budget of acetone, *Geophysical Research Letters*, 39, 5, L01807  
41 10.1029/2011gl050086, 2012.

42 Flöck, O. R., and Andreae, M. O.: Photochemical and non-photochemical formation and destruction of carbonyl  
43 sulfide and methyl mercaptan in ocean waters, *Marine Chemistry*, 54, 11-26, [https://doi.org/10.1016/0304-  
44 4203\(96\)00027-8](https://doi.org/10.1016/0304-4203(96)00027-8), 1996.

45 Galbally, I. E., Lawson, S. J., Weeks, I. A., Bentley, S. T., Gillett, R. W., Meyer, M., and Goldstein, A. H.: Volatile  
46 organic compounds in marine air at Cape Grim, Australia, *Environmental Chemistry*, 4, 178-182,  
47 10.1071/en07024, 2007.

48 Gall, M. P., Davies-Colley, R. J., and Merrilees, R. A.: Exceptional visual clarity and optical purity in a sub-alpine  
49 lake, *Limnology and Oceanography*, 58, 443-451, 10.4319/lo.2013.58.2.0443, 2013.

50 Hall, J. A., and Safi, K.: The impact of in situ Fe fertilisation on the microbial food web in the Southern Ocean,  
51 *Deep Sea Research Part II: Topical Studies in Oceanography*, 48, 2591-2613, [https://doi.org/10.1016/S0967-  
52 0645\(01\)00010-8](https://doi.org/10.1016/S0967-0645(01)00010-8), 2001.

53 Halsey, K. H., Giovannoni, S. J., Graus, M., Zhao, Y., Landry, Z., Thrash, J. C., Vergin, K. L., and de Gouw, J.:  
54 Biological cycling of volatile organic carbon by phytoplankton and bacterioplankton, *Limnology and*  
55 *Oceanography*, 62, 2650-2661, 10.1002/lno.10596, 2017.

56 ISO: ISO 6879: Air Quality, Performance Characteristics and Related Concepts for Air Quality Measuring  
57 Methods, International Organisation for Standardisation, Geneva, Switzerland, 1995.

58 Jacob, D. J., Field, B. D., Jin, E. M., Bey, I., Li, Q. B., Logan, J. A., Yantosca, R. M., and Singh, H. B.:  
59 Atmospheric budget of acetone, *Journal of Geophysical Research-Atmospheres*, 107, 17, 4100  
60 10.1029/2001jd000694, 2002.

1 Johnson, M. T.: A numerical scheme to calculate temperature and salinity dependent air-water transfer velocities  
2 for any gas, *Ocean Sci.*, 6, 913-932, 10.5194/os-6-913-2010, 2010.

3 Jones, A. R., Thomson, D. J., Hort, M., and Devenish, B.: The UK Met Office's next-generation atmospheric  
4 dispersion model, NAME III, in: Proceedings of the 27th NATO/CCMS International Technical Meeting on Air  
5 Pollution Modelling and its Application, edited by: Borrego, C., and Norman, A.-L., Springer, 580–589, 2007.

6 Kettle, A. J., Rhee, T. S., von Hobe, M., Poulton, A., Aiken, J., and Andreae, M. O.: Assessing the flux of different  
7 volatile sulfur gases from the ocean to the atmosphere, *Journal of Geophysical Research*, 106, 12193-12209,  
8 10.1029/2000jd900630, 2001.

9 Kieber, R. J., Zhou, X., and Mopper, K.: Formation of carbonyl compounds from UV-induced photodegradation  
10 of humic substances in natural waters: Fate of riverine carbon in the sea, *Limnology and Oceanography*, 35, 1503-  
11 1515, 10.4319/lo.1990.35.7.1503, 1990.

12 Kiene, R. P.: Production of methanethiol from dimethylsulfoniopropionate in marine surface waters, *Marine*  
13 *Chemistry*, 54, 69-83, [https://doi.org/10.1016/0304-4203\(96\)00006-0](https://doi.org/10.1016/0304-4203(96)00006-0), 1996.

14 Kiene, R. P., and Linn, L. J.: The fate of dissolved dimethylsulfoniopropionate (DMSP) in seawater: tracer studies  
15 using <sup>35</sup>S-DMSP, *Geochimica et Cosmochimica Acta*, 64, 2797-2810, [https://doi.org/10.1016/S0016-](https://doi.org/10.1016/S0016-7037(00)00399-9)  
16 [7037\(00\)00399-9](https://doi.org/10.1016/S0016-7037(00)00399-9), 2000.

17 Kiene, R. P., Linn, L. J., and Bruton, J. A.: New and important roles for DMSP in marine microbial communities,  
18 *Journal of Sea Research*, 43, 209-224, [https://doi.org/10.1016/S1385-1101\(00\)00023-X](https://doi.org/10.1016/S1385-1101(00)00023-X), 2000.

19 Kiene, R. P., Williams, T. E., Esson, K., Tortell, P. D., and Dacey, J. W. H.: Methanethiol Concentrations and  
20 Sea-Air Fluxes in the Subarctic NE Pacific Ocean, American Geophysical Union, Fall meeting, 2017,

21 Kwan, A. J., Crouse, J. D., Clarke, A. D., Shinozuka, Y., Anderson, B. E., Crawford, J. H., Avery, M. A.,  
22 McNaughton, C. S., Brune, W. H., Singh, H. B., and Wennberg, P. O.: On the flux of oxygenated volatile organic  
23 compounds from organic aerosol oxidation, *Geophysical Research Letters*, 33, 10.1029/2006gl026144, 2006.

24 Lana, A., Bell, T. G., Simó, R., Vallina, S. M., Ballabrera-Poy, J., Kettle, A. J., Dachs, J., Bopp, L., Saltzman, E.  
25 S., Stefels, J., Johnson, J. E., and Liss, P. S.: An updated climatology of surface dimethylsulfide concentrations  
26 and emission fluxes in the global ocean, *Global Biogeochemical Cycles*, 25, 10.1029/2010gb003850, 2011.

27 Law, C. S., Brévière, E., de Leeuw, G., Garçon, V., Guieu, C., Kieber, D. J., Konradowitz, S., Paulmier, A.,  
28 Quinn, P. K., Saltzman, E. S., Stefels, J., and von Glasow, R.: Evolving research directions in Surface Ocean-  
29 Lower Atmosphere (SOLAS) science, *Environmental Chemistry*, 10, 1-16, <https://doi.org/10.1071/EN12159>,  
30 2013.

31 Law, C. S., Smith, M. J., Harvey, M. J., Bell, T. G., Cravigan, L. T., Elliott, F. C., Lawson, S. J., Lizotte, M.,  
32 Marriner, A., McGregor, J., Ristovski, Z., Safi, K. A., Saltzman, E. S., Vaattovaara, P., and Walker, C. F.:  
33 Overview and preliminary results of the Surface Ocean Aerosol Production (SOAP) campaign, *Atmos. Chem.*  
34 *Phys.*, 17, 13645-13667, 10.5194/acp-17-13645-2017, 2017.

35 Law, C. S., Woodward, E. M. S., Ellwood, M. J., Marriner, A., Bury, S. J., and Safi, K. A.: Response of surface  
36 nutrient inventories and nitrogen fixation to a tropical cyclone in the southwest Pacific, *Limnology and*  
37 *Oceanography*, 56, 1372-1385, 10.4319/lo.2011.56.4.1372, 2011.

38 Lawson, S. J., Selleck, P. W., Galbally, I. E., Keywood, M. D., Harvey, M. J., Lerot, C., Helmig, D., and Ristovski,  
39 Z.: Seasonal in situ observations of glyoxal and methylglyoxal over the temperate oceans of the Southern  
40 Hemisphere, *Atmos. Chem. Phys.*, 15, 223-240, 10.5194/acp-15-223-2015, 2015.

41 Leck, C., and Rodhe, H.: Emissions of marine biogenic sulfur to the atmosphere of northern Europe, *Journal of*  
42 *Atmospheric Chemistry*, 12, 63-86, 10.1007/bf00053934, 1991.

43 Lee, C. L., and Brimblecombe, P.: Anthropogenic contributions to global carbonyl sulfide, carbon disulfide and  
44 organosulfides fluxes, *Earth-Sci. Rev.*, 160, 1-18, <https://doi.org/10.1016/j.earscirev.2016.06.005>, 2016.

45 Lewis, A. C., Hopkins, J. R., Carpenter, L. J., Stanton, J., Read, K. A., and Pilling, M. J.: Sources and sinks of  
46 acetone, methanol, and acetaldehyde in North Atlantic marine air, *Atmos. Chem. Phys.*, 5, 1963-1974,  
47 10.5194/acp-5-1963-2005, 2005.

48 Liss, P. S., and Johnson, M. T.: *Ocean-Atmosphere Interactions of Gases and Particles*, edited by: Liss, P. S., and  
49 Johnson, M. T., Springer Earth System Sciences, 315 pp., 2014.

50 Lizotte, M., Lévassieur, M., Law, C. S., Walker, C. F., Safi, K. A., Marriner, A., and Kiene, R. P.:  
51 Dimethylsulfoniopropionate (DMSP) and dimethyl sulfide (DMS) cycling across contrasting biological hotspots  
52 of the New Zealand subtropical front, *Ocean Sci.*, 13, 961-982, 10.5194/os-13-961-2017, 2017.

53 Malin, G.: Sulphur, climate and the microbial maze, *Nature*, 387, 857-858, 10.1038/43075, 1997.

54 Marandino, C. A., De Bruyn, W. J., Miller, S. D., Prather, M. J., and Saltzman, E. S.: Oceanic uptake and the  
55 global atmospheric acetone budget, *Geophysical Research Letters*, 32, 10.1029/2005gl023285, 2005.

56 Marandino, C. A., De Bruyn, W. J., Miller, S. D., and Saltzman, E. S.: Eddy correlation measurements of the  
57 air/sea flux of dimethylsulfide over the North Pacific Ocean, *Journal of Geophysical Research: Atmospheres*, 112,  
58 10.1029/2006jd007293, 2007.

59 Nemecek-Marshall, M., Wojciechowski, C., Kuzma, J., Silver, G. M., and Fall, R.: Marine *Vibrio* species produce  
60 the volatile organic compound acetone, *Appl Environ Microbiol*, 61, 44-47, 1995.



1 Nemecek-Marshall, M., Wojciechowski, C., Wagner, W. P., and Fall, R.: Acetone formation in the *Vibrio* family:  
2 a new pathway for bacterial leucine catabolism, *J Bacteriol*, 181, 7493-7499, 1999.

3 Nodder, S. D., Chiswell, S. M., and Northcote, L. C.: Annual cycles of deep-ocean biogeochemical export fluxes  
4 in subtropical and subantarctic waters, southwest Pacific Ocean, *Journal of Geophysical Research: Oceans*, 121,  
5 2405-2424, 10.1002/2015jc011243, 2016.

6 Pan, X., Underwood, J. S., Xing, J. H., Mang, S. A., and Nizkorodov, S. A.: Photodegradation of secondary  
7 organic aerosol generated from limonene oxidation by ozone studied with chemical ionization mass spectrometry,  
8 *Atmos. Chem. Phys.*, 9, 3851-3865, 10.5194/acp-9-3851-2009, 2009.

9 Quinn, P. K., and Bates, T. S.: The case against climate regulation via oceanic phytoplankton sulphur emissions,  
10 *Nature*, 480, 51-56, 10.1038/nature10580, 2011.

11 Read, K. A., Carpenter, L. J., Arnold, S. R., Beale, R., Nightingale, P. D., Hopkins, J. R., Lewis, A. C., Lee, J. D.,  
12 Mendes, L., and Pickering, S. J.: Multiannual Observations of Acetone, Methanol, and Acetaldehyde in Remote  
13 Tropical Atlantic Air: Implications for Atmospheric OVOC Budgets and Oxidative Capacity, *Environmental  
14 Science & Technology*, 46, 11028-11039, 10.1021/es302082p, 2012.

15 Safi, K. A., Griffiths, F. B., and Hall, J. A.: Microzooplankton composition, biomass and grazing rates along the  
16 WOCE SR3 line between Tasmania and Antarctica, *Deep Sea Research Part I: Oceanographic Research Papers*,  
17 54, 1025-1041, <https://doi.org/10.1016/j.dsr.2007.05.003>, 2007.

18 Sander, R.: Compilation of Henry's law constants (version 4.0) for water as solvent, *Atmos. Chem. Phys.*, 15,  
19 4399-4981, 10.5194/acp-15-4399-2015, 2015.

20 Schlundt, C., Tegtmeier, S., Lennartz, S. T., Bracher, A., Cheah, W., Krüger, K., Quack, B., and Marandino, C.  
21 A.: Oxygenated volatile organic carbon in the western Pacific convective center: ocean cycling, air-sea gas  
22 exchange and atmospheric transport, *Atmos. Chem. Phys.*, 17, 10837-10854, 10.5194/acp-17-10837-2017, 2017.

23 Simó, R., and Pedrós-Alió, C.: Short-term variability in the open ocean cycle of dimethylsulfide, *Global  
24 Biogeochemical Cycles*, 13, 1173-1181, 10.1029/1999gb900081, 1999.

25 Sinha, V., Williams, J., Meyerhofer, M., Riebesell, U., Paulino, A. I., and Larsen, A.: Air-sea fluxes of methanol,  
26 acetone, acetaldehyde, isoprene and DMS from a Norwegian fjord following a phytoplankton bloom in a  
27 mesocosm experiment, *Atmospheric Chemistry and Physics*, 7, 739-755, 2007.

28 Smith, M. J., Walker, C. F., Bell, T. G., Harvey, M. J., Saltzman, E. S., and Law, C. S.: Gradient flux  
29 measurements of sea-air DMS transfer during the Surface Ocean Aerosol Production (SOAP) experiment, *Atmos.  
30 Chem. Phys.*, 18, 5861-5877, 10.5194/acp-18-5861-2018, 2018.

31 Somogyi, M.: Notes on Sugar Determination, *Journal of Biological Chemistry*, 70, 599-612, 1926.

32 Somogyi, M.: Notes on Sugar Determination, *Journal of Biological Chemistry*, 195, 19-23, 1952.

33 Sun, J., Todd, J. D., Thrash, J. C., Qian, Y., Qian, M. C., Temperton, B., Guo, J., Fowler, E. K., Aldrich, J. T.,  
34 Nicora, C. D., Lipton, M. S., Smith, R. D., De Leenheer, P., Payne, S. H., Johnston, A. W. B., Davie-Martin, C.  
35 L., Halsey, K. H., and Giovannoni, S. J.: The abundant marine bacterium *Pelagibacter* simultaneously catabolizes  
36 dimethylsulfoniopropionate to the gases dimethyl sulfide and methanethiol, *Nature Microbiology*, 1, 16065,  
37 10.1038/nmicrobiol.2016.65  
38 <https://www.nature.com/articles/nmicrobiol201665#supplementary-information>, 2016.

39 Taddei, S., Toscano, P., Gioli, B., Matese, A., Miglietta, F., Vaccari, F. P., Zaldei, A., Custer, T., and Williams,  
40 J.: Carbon Dioxide and Acetone Air-Sea Fluxes over the Southern Atlantic, *Environmental Science &  
41 Technology*, 43, 5218-5222, 10.1021/es8032617, 2009.

42 Tanimoto, H., Kameyama, S., Iwata, T., Inomata, S., and Omori, Y.: Measurement of Air-Sea Exchange of  
43 Dimethyl Sulfide and Acetone by PTR-MS Coupled with Gradient Flux Technique, *Environmental Science &  
44 Technology*, 48, 526-533, 10.1021/es4032562, 2014.

45 Tyndall, G. S., and Ravishankara, A. R.: Atmospheric oxidation of reduced sulfur species, *International Journal  
46 of Chemical Kinetics*, 23, 483-527, 10.1002/kin.550230604, 1991.

47 Walker, C. F., Harvey, M. J., Smith, M. J., Bell, T. G., Saltzman, E. S., Marriner, A. S., McGregor, J. A., and  
48 Law, C. S.: Assessing the potential for dimethylsulfide enrichment at the sea surface and its influence on air-sea  
49 flux, *Ocean Sci.*, 12, 1033-1048, 10.5194/os-12-1033-2016, 2016.

50 Warneke, C., and de Gouw, J. A.: Organic trace gas composition of the marine boundary layer over the northwest  
51 Indian Ocean in April 2000, *Atmospheric Environment*, 35, 5923-5933, 2001.

52 Williams, T. L., Adams, N. G., and Babcock, L. M.: Selected ion flow tube studies of  $\text{H}_3\text{O}^+(\text{H}_2\text{O})_{0.1}$  reactions with  
53 sulfides and thiols, *International Journal of Mass Spectrometry and Ion Processes*, 172, 149-159,  
54 [https://doi.org/10.1016/S0168-1176\(97\)00081-5](https://doi.org/10.1016/S0168-1176(97)00081-5), 1998.

55 Williams, J., Holzinger, R., Gros, V., Xu, X., Atlas, E., and Wallace, D. W. R.: Measurements of organic species  
56 in air and seawater from the tropical Atlantic, *Geophysical Research Letters*, 31, 5, L23s06  
57 10.1029/2004gl020012, 2004.

58 Williams, J., Custer, T., Riede, H., Sander, R., Jöckel, P., Hoor, P., Pozzer, A., Wong-Zehnpfennig, S., Hosaynali  
59 Beygi, Z., Fischer, H., Gros, V., Colomb, A., Bonsang, B., Yassaa, N., Peeken, I., Atlas, E. L., Waluda, C. M.,  
60 van Aardenne, J. A., and Lelieveld, J.: Assessing the effect of marine isoprene and ship emissions on ozone, using

1 modelling and measurements from the South Atlantic Ocean, *Environmental Chemistry*, 7, 171-182,  
2 doi:10.1071/EN09154, 2010.

3 Yang, M., Beale, R., Liss, P., Johnson, M., Blomquist, B., and Nightingale, P.: Air-sea fluxes of oxygenated  
4 volatile organic compounds across the Atlantic Ocean, *Atmos. Chem. Phys.*, 14, 7499-7517, 10.5194/acp-14-  
5 7499-2014, 2014a.

6 Yang, M., Blomquist, B. W., and Nightingale, P. D.: Air-sea exchange of methanol and acetone during HiWinGS:  
7 Estimation of air phase, water phase gas transfer velocities, 119, 7308-7323, 10.1002/2014jc010227, 2014b.

8 Yoch, D. C.: Dimethylsulfoniopropionate: Its Sources, Role in the Marine Food Web, and Biological Degradation  
9 to Dimethylsulfide, 68, 5804-5815, 10.1128/AEM.68.12.5804-5815.2002, *Applied and Environmental*  
10 *Microbiology*, 2002.

11 Yvon, S. A., Cooper, D. J., Koropalov, V., and Saltzman, E. S.: Atmospheric hydrogen sulfide over the equatorial  
12 Pacific (SAGA 3), *Journal of Geophysical Research: Atmospheres*, 98, 16979-16983, 10.1029/92jd00451, 1993.

13 Zhou, X., and Mopper, K.: Photochemical production of low-molecular-weight carbonyl compounds in seawater  
14 and surface microlayer and their air-sea exchange, *Marine Chemistry*, 56, 201-213,  
15 [https://doi.org/10.1016/S0304-4203\(96\)00076-X](https://doi.org/10.1016/S0304-4203(96)00076-X), 1997.

16  
17  
18

1  
2  
3  
4  
5

**Table 1. Results of the DMS bag sample intercomparison study undertaken during the SOAP voyage. Note that a 1 s PTR-MS dwell time for m/z 63 and 66 was used during the intercomparison compared to the 10 s during ambient measurements; as such the PTR-MS standard deviation reported here is expected to be ~3 times higher than during ambient measurements. Total refers to the ambient DMS + spiked tri-deuterated DMS bag sample on DOY 65.**

DOY	Comparison	DMS (ppt) av ± stdev			DMS ratios		
		GC-SCD	PTR-MS	mesoCIMS	GC-SCD /PTR-MS	PTR-MS /mesoCIMS	GC-SCD /mesoCIMS
64	<i>Standard (dry)</i>	354 ± 6	339 ± 64	n/a	1.04 ± 0.2	n/a	n/a
65	<i>Standard (dry)</i>	289 ± 2	262 ± 43	383 ± 30	1.1 ± 0.18	0.68 ± 0.12	0.75 ± 0.06
64	<i>Ambient</i>	168 ± 5	158 ± 49	n/a	1.06 ± 0.33	n/a	n/a
65	<i>Ambient</i>	n/a	127 ± 43	141 ± 5	n/a	0.90 ± 0.30	n/a
	<i>+tri-deuterated DMS</i>	n/a	197 ± 49	260 ± 2	n/a	0.76 ± 0.19	n/a
	<i>Total</i>	323 ± 9	324 ± 66	401 ± 6	1.0 ± 0.2	0.81 ± 0.16	0.81 ± 0.03

6  
7  
8  
9

**Table 2. MeSH<sub>a</sub>, DMS<sub>a</sub> and acetone<sub>a</sub> measured with PTR-MS during the SOAP voyage, reaction rate constant for OH and calculated lifetime with respect to OH**

	Mean (range) ppt	k <sub>OH</sub> * (cm <sup>3</sup> molecule <sup>-1</sup> s <sup>-1</sup> )	Lifetime (days)
MeSH	18 (BDL – 65)	3.40E <sup>-11</sup>	0.4
DMS	208 (BDL – 957)	1.29E <sup>-11</sup>	1
acetone	237 (54-1508)	2.20E <sup>-13</sup>	60

10  
11  
12

BDL= below detection limit

\*Reaction rate constants from Atkinson 1997 (MeSH), Berresheim et al 1987 (DMS) and Atkinson 1986 (acetone)

**Table 3. Pearson correlations between DMS<sub>a</sub> and MeSH<sub>a</sub> and acetone<sub>a</sub> which are significant at 95% confidence interval. Land influenced data removed (acetone)**

		Slope (p-value)	R <sup>2</sup>
DMS vs MeSH	All data (n=266)	0.07 (<0.0001)	0.3
	B2 (n=98)	0.13 (<0.0001)	0.5
	B3 (n=76)	0.03 (0.001)	0.1
DMS vs acetone	All data (n=1301)	0.30 (<0.0001)	0.1
	B1 (n=883)	0.19 (<0.0001)	0.1
	B2 (n=122)	1.1 (<0.0001)	0.2
Acetone vs MeSH	All data (n=265)	0.02 (<0.0001)	0.1
	B3 (n=76)	0.06 (0.03)	0.1

1  
2  
3  
4

**Table 4. MeSH and DMS fluxes calculated using the nocturnal buildup method (NBM), compared with DMS flux measured using eddy covariance (EC) method (Bell et al., 2015). The  $\pm$  values on the MeSH and DMS flux are due to the standard deviation (std dev) of the MBL height.**

Bloom	DOY	MeSH ppt hr <sup>-1</sup>	DMS ppt hr <sup>-1</sup>	MeSH/MeSH+DMS (%)	Flux MeSH $\mu\text{mol m}^{-2} \text{day}^{-1}$	NBM Flux DMS $\mu\text{mol m}^{-2} \text{day}^{-1}$	EC Flux DMS mean $\pm$ std dev
Just prior to B2	52.2 - 52.7	3 $\pm$ 1	11 $\pm$ 3	24	3.5 $\pm$ 2.0	12.7 $\pm$ 7.4	7.6 $\pm$ 4.8
B2	54.2 - 54.4	5 $\pm$ 1	16 $\pm$ 3	23	5.8 $\pm$ 3.4	18.5 $\pm$ 10.7	26.4 $\pm$ 9.7
B3a	60.2 - 60.4	4 $\pm$ 2	27 $\pm$ 4	14	4.8 $\pm$ 2.8	31.0 $\pm$ 17.9	29.4 $\pm$ 8.2

5  
6  
7

**Table 5. MeSH flux from this and previous studies (voyage averages)**

Location	MeSH flux ( $\mu\text{mol m}^{-2} \text{day}^{-1}$ )	Flux MeSH/MeSH+DMS (%)	Reference
Baltic sea	0.2	5%	Leck and Rodhe., 1991
Kattegat sea	0.8	4%	
North Sea	1.6	11%	
North/South Atlantic	1.2	16%	Kettle et al., 2001
Northeast subarctic Pacific	Not reported	~15%	Kiene et al., 2017
South West Pacific	4.7	20%	This study

8  
9  
10  
11  
12  
13  
14

**Table 6. Spearman rank correlations between acetone<sub>a</sub>, DMS<sub>a</sub> and MeSH<sub>a</sub> and biogeochemical parameters, using data from the 14 February 2012 – 4 March 2012 (acetone<sub>a</sub>, DMS<sub>a</sub>) and 20 February 2012 – 4 March 2012 (MeSH<sub>a</sub>). Correlations shown are significant at 95% confidence interval (CI). Correlation coefficient (and p-value) are shown. No entry indicates there was no correlation at 95% CI. Land influenced acetone<sub>a</sub> data excluded (see text for details).**

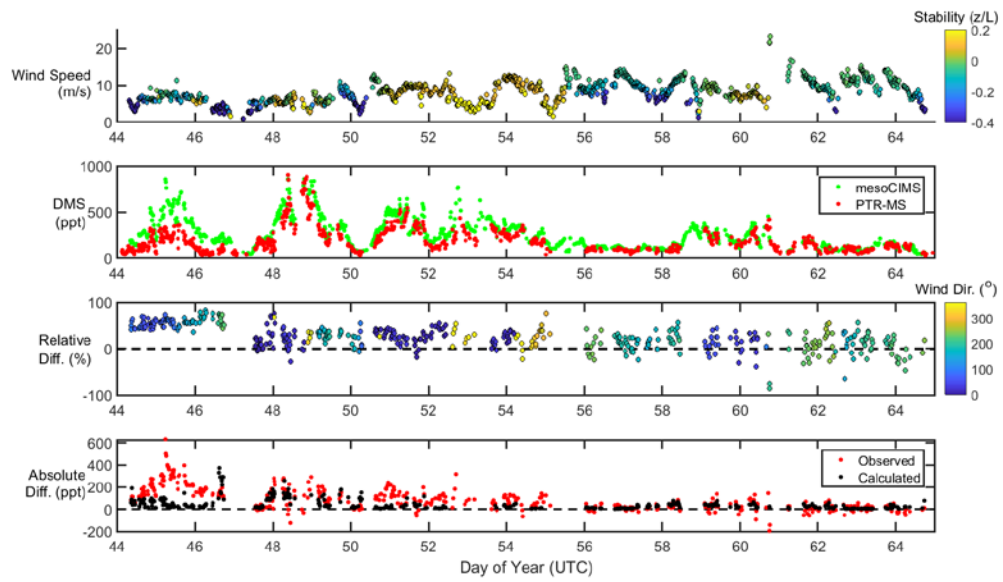
	Acetone <sub>a</sub>	DMS <sub>a</sub>	MeSH <sub>a</sub>
<b>Positive correlations</b>			
salinity (psu)	0.55 (0.005) n=25		
sea temperature (°C)	0.77 (<0.0001) n=25		
beta -660 backscatter ( $\text{m}^{-2} \text{sr}^{-1}$ )	0.67 (0.0004) n=25		
DMS <sub>sw</sub> (nM)	0.49 (0.025) n=21	0.73 (0.0002) n=22	0.59 (0.011) n=18
Chla/mixed layer depth	0.50 (0.014) n=25		
particulate nitrogen ( $\text{mg m}^{-3}$ )		0.79 (0.048) n=7	
cryptophyte algae (cells mL <sup>-1</sup> )	0.47 (0.019) n=25		
eukaryotic picoplankton (cells mL <sup>-1</sup> )	0.48 (0.016)		

	n=25		
DMSPt (nmolL <sup>-1</sup> )		0.54 (0.011) n=22	0.59 (0.014) n=17
DMSPP (nmolL <sup>-1</sup> )		0.56 (0.007) n=22	0.53 (0.032) n=17
CDOM (ppb)	0.48 (0.041) n=20		
HMW reducing sugars (µg L <sup>-1</sup> )	0.67 (0.011) n=14		
<b>Negative correlations</b>			
Chla/backscatter 660	-0.47 (0.019) n=25		
mixed layer depth (m)	-0.66 (0.0005) n=25		
dissolved oxygen (µmol kg <sup>-1</sup> )	-0.45 (0.030) n=24		
phosphate (µmolL <sup>-1</sup> )	-0.54 (0.006) n=25		
nitrate (µmolL <sup>-1</sup> )	-0.60 (0.002) n=25		
silicate (µmolL <sup>-1</sup> )	-0.50 (0.012) n=25	-0.43 (0.031) n=26	
monounsaturated fatty acids (µg/L <sup>-1</sup> )	-0.82 (0.007) n=10		

1

2

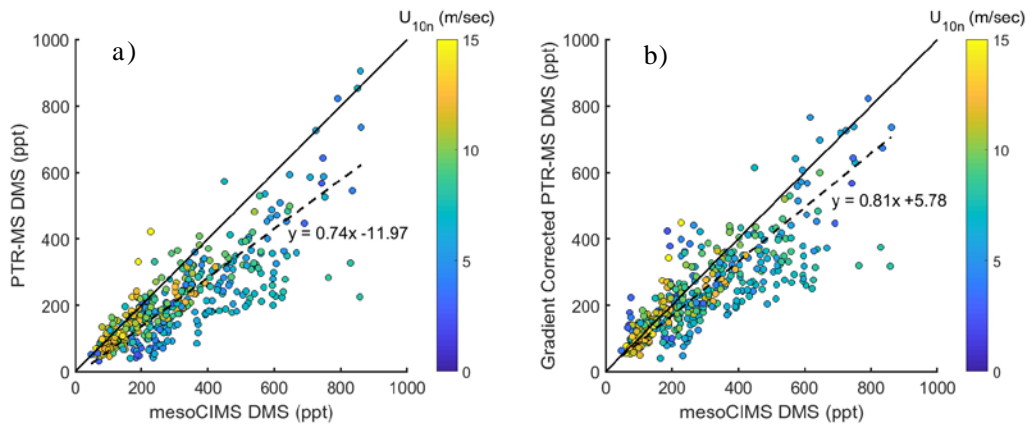
1  
2



3  
4  
5  
6  
7

**Figure 1** From top to bottom, wind speed and stability, DMS<sub>a</sub> measurements from mesoCIMS and PTR-MS, relative difference (normalised to mesoCIMS) according to absolute wind direction, and absolute observed and calculated difference between mesoCIMS and PTR-MS, taking into account the expected DMS concentration gradient (Eq. 1)

1



2

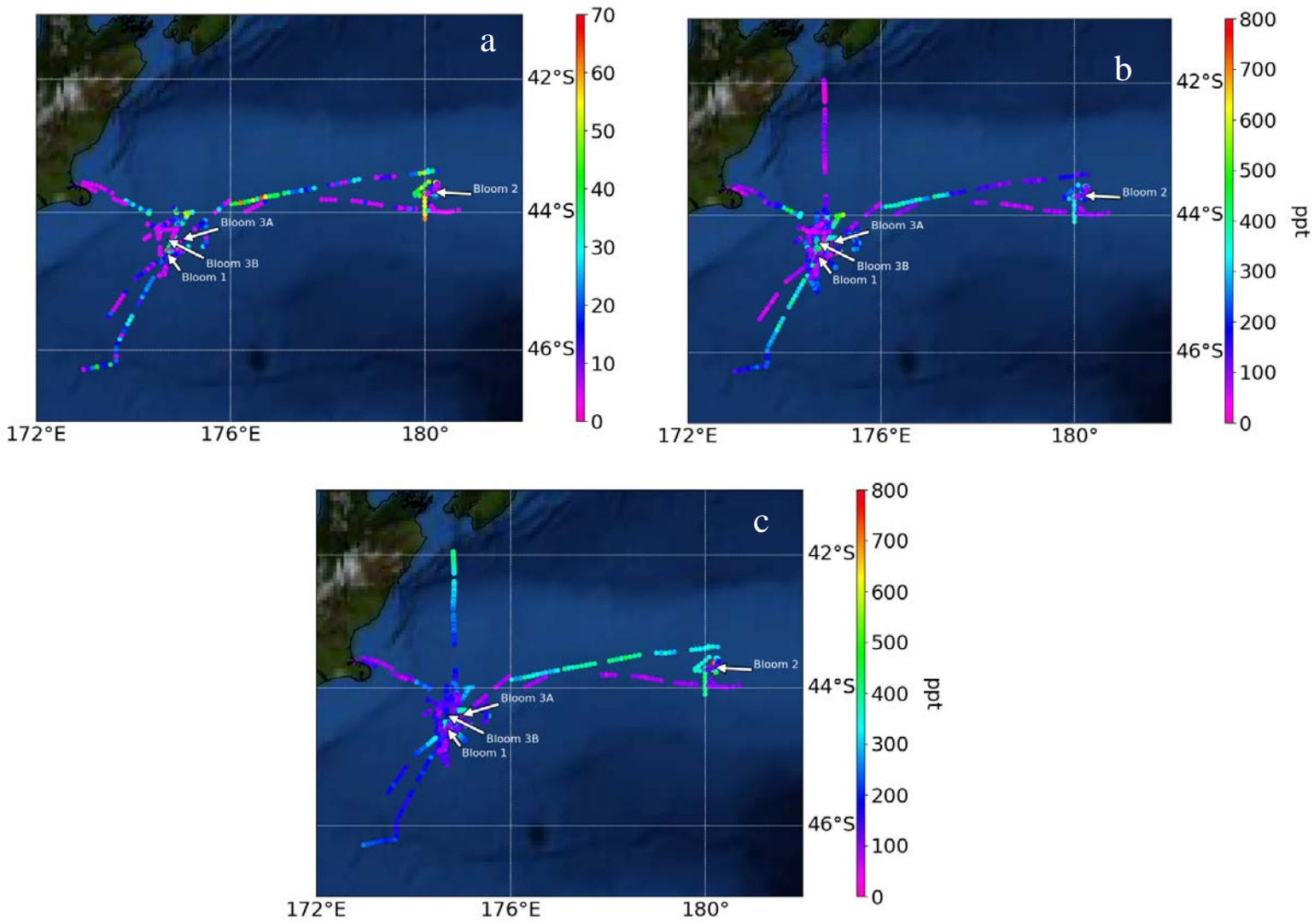
3 **Fig 2 a) DMS<sub>a</sub> measured by mesoCIMS (x) and PTR-MS (y) b) mesoCIMS (x) and PTR-MS (y) DMS data corrected**  
4 **for the expected concentration gradient (observed PTR-MS DMS + calculated delta DMS). Dashed lines represent the**  
5 **reduced major axis regression and solid lines represent a 1:1 relationship.**

6

7

8

9

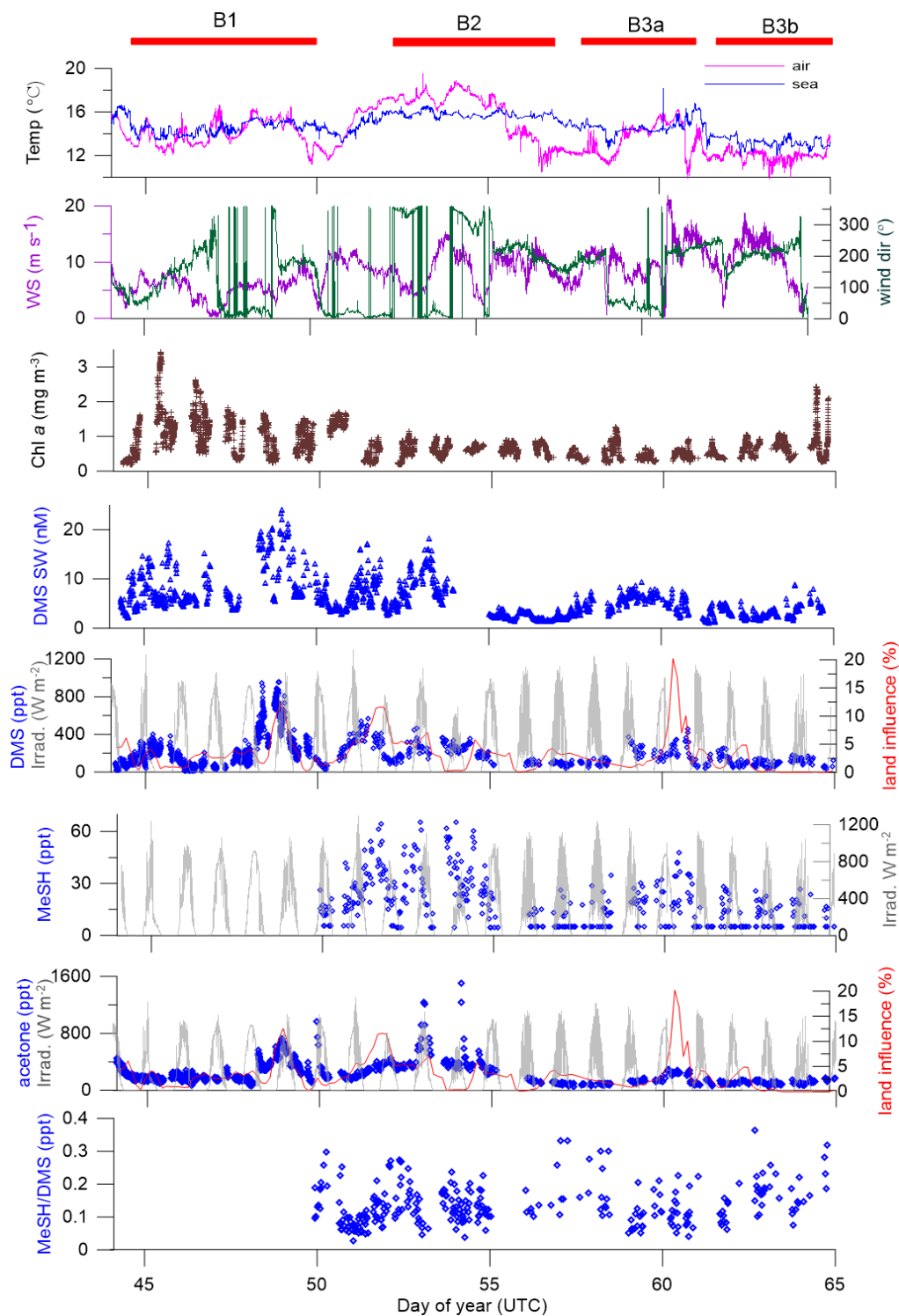


1

2 **Fig 3 Atmospheric mixing ratios of (a)MeSHa, (b) DMSa and (c) acetonea as function of the voyage track. Location of**  
 3 **the blooms are shown.**

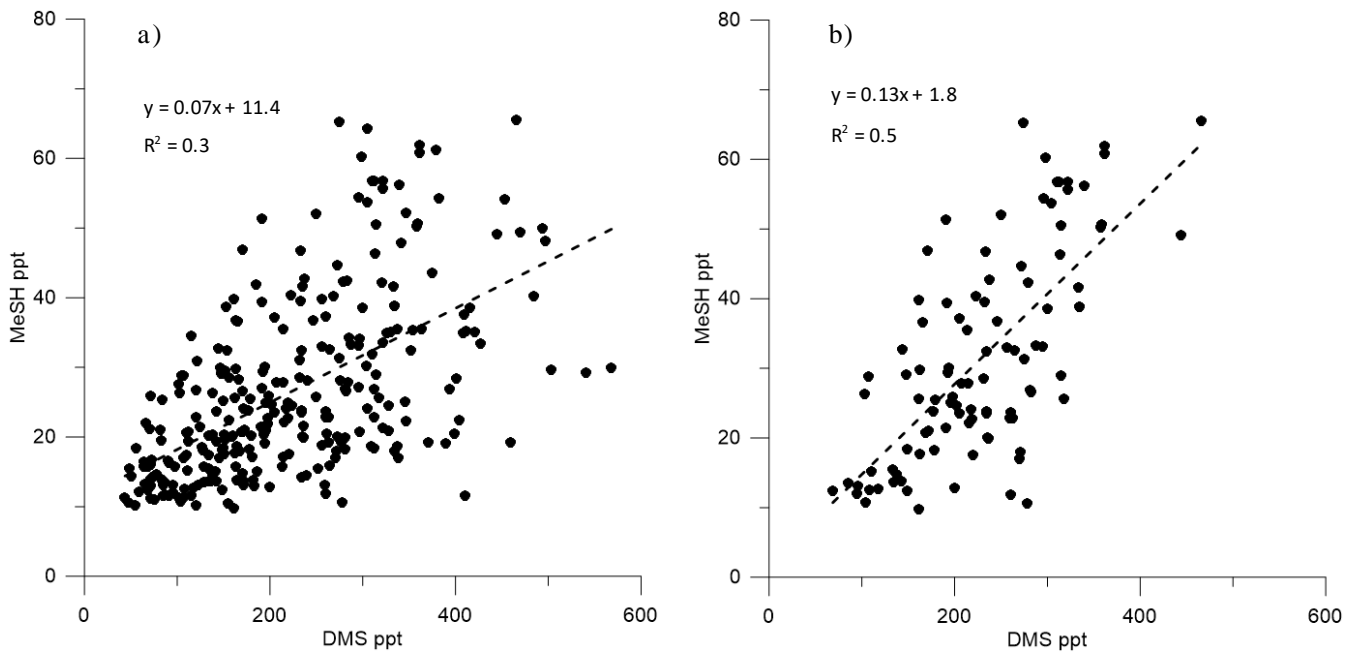
4





1  
2  
3  
4  
5

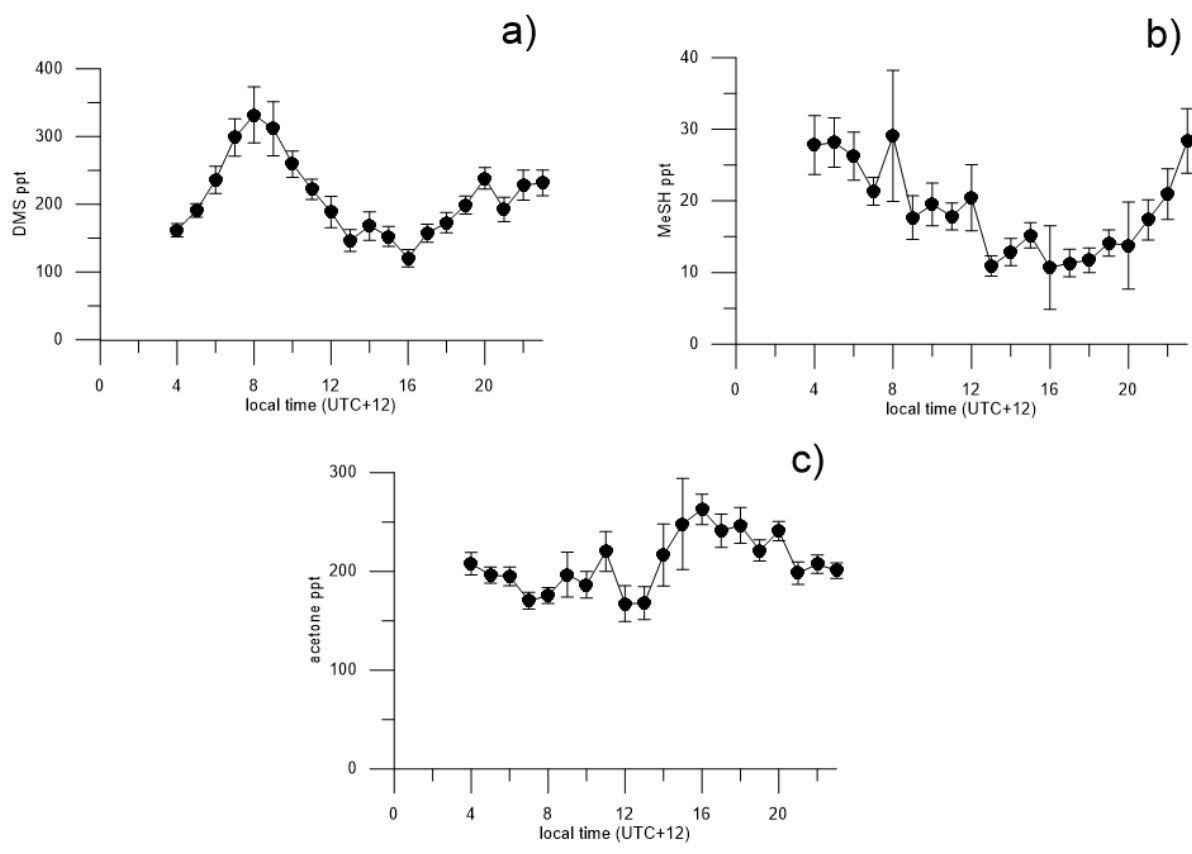
Figure 4 -times series of measurements during the SOAP voyage according to DOY. Atmospheric DMS and MeSH measurements below detection limit have had half detection limit substituted. WS = wind speed, wind dir = wind direction, Irrad. = irradiance, Chl a =chlorophyll a



1

2 **Fig 5. Correlation between a) DMS<sub>a</sub> and MeSH<sub>a</sub> all data (DOY 49 onwards), b) DMS<sub>a</sub> and MeSH<sub>a</sub> bloom (B2) only**

3



1  
2  
3  
4  
5  
6  
7  
8

**Fig 6. Diurnal cycles of a) DMS, b) MeSH, c) acetone with land influenced data removed. Average values from 0:00-3:00 are excluded because of lower data collection during this period, due to calibrations and zero air measurements**